

We are IntechOpen, the world's leading publisher of Open Access books Built by scientists, for scientists

6,900

Open access books available

185,000

International authors and editors

200M

Downloads

Our authors are among the

154

Countries delivered to

TOP 1%

most cited scientists

12.2%

Contributors from top 500 universities



WEB OF SCIENCE™

Selection of our books indexed in the Book Citation Index
in Web of Science™ Core Collection (BKCI)

Interested in publishing with us?
Contact book.department@intechopen.com

Numbers displayed above are based on latest data collected.
For more information visit www.intechopen.com



A Novel 4-DOF Parallel Manipulator H4

Jinbo Wu¹ and Zhouping Yin²

¹ Traffic Science & Engineering College

² State Key Laboratory of Digital Manufacturing Equipment and Technology
Huazhong University of Science & Technology
China

1. Introduction

Parallel manipulators have the advantages of high stiffness and low inertia compared to serial mechanisms. Based on the Steward-Gough platform architecture, a lot of 6-DOF mechanical devices have been proposed. The 6-DOF parallel manipulators suffer from a small workspace, complex mechanical design, and difficult motion generation and control due to their complex kinematic analysis. To overcome these shortcomings, the *limited-DOF manipulator*, which has fewer than 6 DOFs, can be found in many production lines. It is clear today that most attention has been paid to 3-DOF family among the limited-DOF parallel manipulators (Carretero, 2000). However, in many industrial situations, there is a need for equipment providing more than 3-DOFs. For example, for most pick-and-place applications in semiconductor manufacturing, at least 4 DOFs are required (3 translation to move the carried die from one point to the other, 1 rotation to adjust the orientation in its final location). A new family of 4-dof parallel manipulators called H4 that could be useful for high-speed pick-and-place applications is proposed by Pierrot and Company (Pierrot, 1999). The H4 manipulator offers 3 DOFs in translation and 1 DOF in rotation about a given axis. The H4 manipulator is useful for high-speed handling in robotics and milling in machine-tool industry since it is a fully-parallel mechanism with no passive chain and able to provide high performance in terms of speed and acceleration.

This chapter discusses the kinematic analysis of the H4 manipulator. In section 2, synthesis methods for designing H4 are presented, and various possible mechanical architectures of the parallel manipulator are exposed. Section 3 discusses the inverse and forward kinematics problem of H4. Section 4 deals with singularity analysis of H4 utilizing line geometry tools and screw theory. Section 5 concludes this chapter by providing the development tendency of the parallel manipulators.

2. Structural synthesis and architectures

2.1 General concept of H4

Parallel manipulators are constituted of a moving platform that is connected to a fixed base by several chains (limbs). Generally, the number of limbs is equal to the degrees of freedom (DOF) of the moving platform such that each limb is driven by no more than one actuator and all actuators can be mounted on or near the fixed base. By acting on the limbs the

Source: Parallel Manipulators, Towards New Applications, Book edited by: Huapeng Wu, ISBN 978-3-902613-40-0, pp. 506, April 2008, I-Tech Education and Publishing, Vienna, Austria

platform pose (position and orientation) is controlled. Moreover, if the actuators are locked, the manipulator will become an isostatic structure in which all the legs carry the external loads applied to the platform. This feature makes the parallel manipulators with high stiffness possible throughout the whole space. From the first ideas proposed by Gough (Gough, 1956) or Steward (Steward, 1965), a lot of interesting mechanical devices or design methods have been extensively studied. In the beginning, many structures were based on the ingenuity of the researchers and not on a systematic approach. Subsequently, a new research domain called *structure (or type) synthesis* was proposed, in which various methodologies were tried to generate all the structures that have a desired kinematic performance. The most widely used synthesis approaches (and their variants) are *graph theory*, *group theory* and *screw theory* (Merlet, 2006). In this section, we will not discuss these theoretical problems, but focus on the structure generation of H4.

The 6-DOF parallel manipulators generally suffer from a small workspace, complex mechanical design and difficult motion generation and control due to their complex kinematic analysis. To overcome these shortcomings, new structures for parallel manipulators having less than 6-DOF (which are called limited-DOF manipulators in this chapter, although many of these new structures were known well before) are explored. There is an overriding motivation behind such efforts: limited-DOF manipulators may be needed for many applications. For example, parallel wrists need only three rotational DOFs. It is clear today that most attention has been paid to 3-DOF family among the limited-DOF parallel manipulators (Gosselin & Angeles, 1989; Agrawal et al., 1995; Gosselin & St-Pierre, 1997; Fattah & Kasaei, 2000; Gregorio, 2001). However, in many industrial situations, there is a need for equipment providing more than 3 DOFs arranged in parallel and based on simpler arrangements than 6-DOF structures. The reference (Cheung et al., 2002) developed a 4-DOF parallel manipulator E4 which could be used in a semiconductor packaging system. It is in the early 80's when Reymond Clavel comes up with the brilliant idea of using parallelograms to build a parallel robot with three translational and one rotational degree of freedom (Benevise, 2001). Contrary to opinions published elsewhere, his inspiration was truly original and does not come from any parallel mechanism patents. Professor Clavel called his creation the Delta robot. The new family of 4-DOF parallel manipulators called H4 that could be useful for high-speed pick-and-place applications is just based on the idea of Delta structure (Pierrot & Company, 1999; Company & Pierrot, 1999). The prototype built in the Robotics Department of LIRMM can reach 10g accelerations and velocities higher than 5m/s (Robotics Department of LIRMM).

2.1.1 Delta structure

Even if an incredibly large number of different structures have been proposed by academic researchers in the last 30 years, most of these that are used widely in industry can be classified into two basic types: the Delta structure and the so-called "hexapod" with 6 U-P-S chains in parallel (U-P-S: Universal-Prismatic-Spherical). This may be a result of either the exceptional simplicity of the Delta 3-DOF solution, or the enormous research effort dedicated to "hexapod" (Company, 1999).

The basic idea behind the Delta parallel robot design is the use of parallelograms. A parallelogram allows an output link to remain at a fixed orientation with respect to an input link. The use of three such parallelograms restrain completely the orientation of the mobile platform which remains only with three purely translational degrees of freedom. The input

links of the three parallelograms are mounted on rotating levers via revolute joints. The revolute joints of the rotating levers are actuated in two different ways: with rotational (DC or AC servo) motors or with linear actuators. Finally, a fourth leg is used to transmit rotary motion from the base to an end-effector mounted on the mobile platform. Fig.1 shows the most famous Delta robot with three translation degrees of freedom, which was initially developed at École Polytechnique from Lausanne by Clavel (Clavel, 1988). All the kinematic chains of this robot are of the $RRPaR$ type: a motor makes a revolute joint rotate about an axis \mathbf{w} . On this joint is a lever, at the end of which another joint of the R type is set, with axis parallel to \mathbf{w} . A parallelogram Pa is fixed to this joint, and allows translation in the direction parallel to \mathbf{w} . At the end of this parallelogram is a joint of the R type, with axis parallel to \mathbf{w} , and which is linked to the end effector.

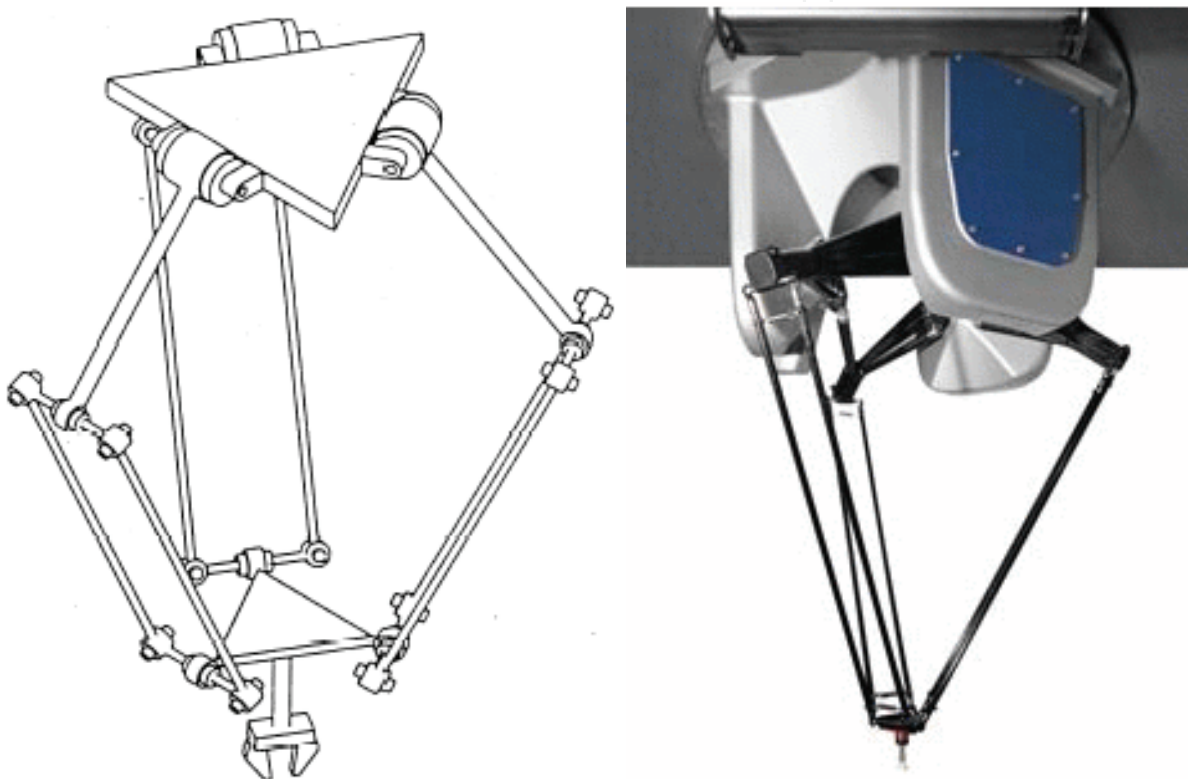


Fig.1. The Delta structure proposed by Prof. Clavel and one of its industrial version, the CE33 (courtesy of SIG Pack Systems)

The Delta robot is firstly marked by the two Swiss brothers Marc-Olivier and Pascal Demarex who created the Demarex company (Bonev, 2001). The joint-and-loop graph of the Delta robot and one of its equivalent structures are shown in Fig.2, where P, R and S represent prismatic, revolute and spherical joint respectively. The displacement of the end-effector of the Delta robot is the result of the movement of the three articulated arms mounted on the base, each of which are connected to a pair of parallel rods. The three orientations are eliminated by joining the rods in a common termination and the three parallelograms ensure the stability of the end-effector. It is noted that the rotary actuator and lever part of the Delta could be replaced by a linear actuator, as suggested by Clavel itself and Zobel (Zobel, 1996). This type of Delta is sometime called a Linapod or a linear Delta.

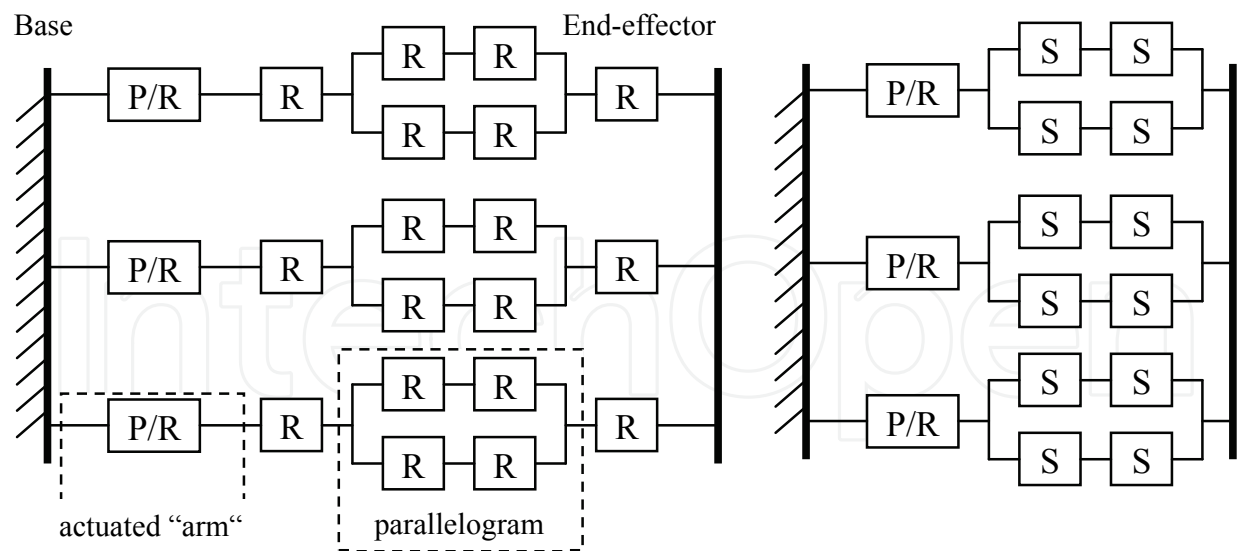


Fig.2. Joint-and-loop graph of the Delta robot and one of its equivalent structure

2.1.2 Structure derivation of H4

H4 is based on 4 independent kinematic chains between the base and the nacelle, each chain is actuated where each actuator is fixed on the base (Pierrot & Company, 1999; Company & Pierrot, 1999). Such technological and conceptual ideas have already proven their efficiency on high-speed equipment for the Delta robot. So, knowing the advantages of this family of mechanisms, it is interesting to recall a few important design features of the Delta robot. The Delta robot is based on three actuated linear or rotational joints, and three pairs of rods equipped with ball joints at each end. As a matter of fact, two ball joints on each rod introduce an internal DOF for the rod which can rotate about its own axis. An arrangement such as the one depicted in Fig.3 suppresses these internal DOF and keeps the same global behaviour. To go a little further, it is possible to consider each pair of rods (that is: two U-S chains parallel one to the other) as equivalent to a unique rod equipped with universal joints at each extremity. The admissible motions for both chains are not exactly the same, but they can be regarded as “equivalent” in terms of number and type of degrees of motion.

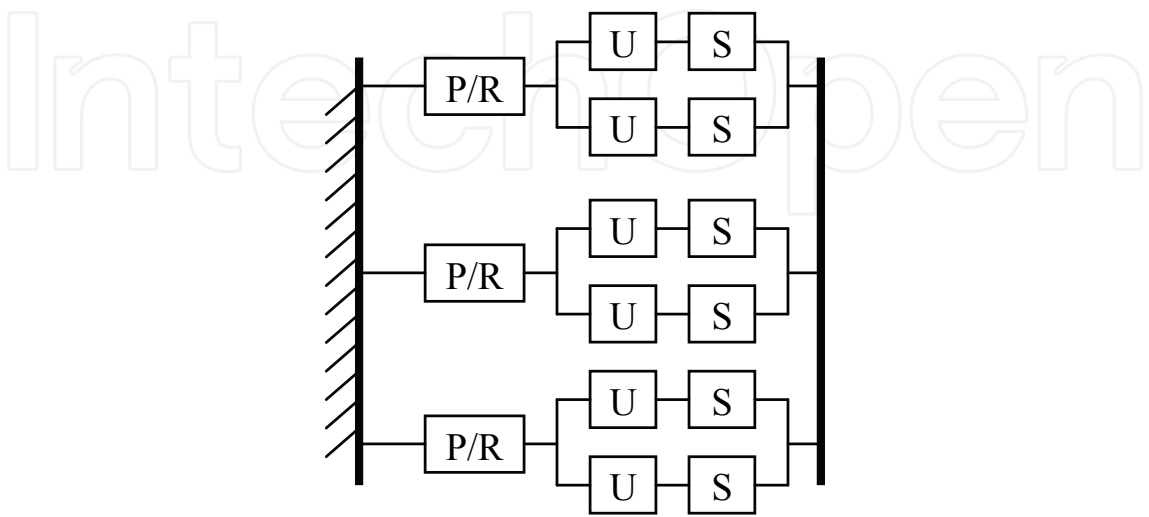


Fig.3. The structure of a Delta robot with no internal DOF

In order to define the basic principle of a 4-DOF mechanism, the classical kinematics formulas can be used. For a mechanism with a “closed loop” (a chain going from ground to the nacelle, and then back to ground), its mobility is given by:

$$m = \sum_{i=1}^{N_l} dof_i - 6L \quad (1)$$

where L is the number of loops; dof_i is the number of DOF of the i th link; N_l is the number of links.

For a fully-parallel 4-DOF mechanisms involving no passive chain, $L = 3$ and $m = 4$. Thus:

$$\sum_{i=1}^{N_l} dof_i = 4 + (6 \times 3) = 22$$

The four P-U-U chains provide: $4 \times 5 = 20dof$. Thus each additional joint must be only 1 DOF joint. Two rotational joints can be used because such joints are extremely easy to manufacture with good accuracy at low cost. So the arrangement shown in Fig.3 are created, each pair is connected to the nacelle by an R joint. Note that the actuated prismatic joints can be replaced by actuated rotational joints, and that the U-U chains can be replaced by (U-S)₂ chains as well (shown in Fig.3(b)). To date, the conditions for a 4-DOF machine have been set up. The conditions to be fulfilled for obtaining 3 translations and 1 rotation about a given axis should be provided.

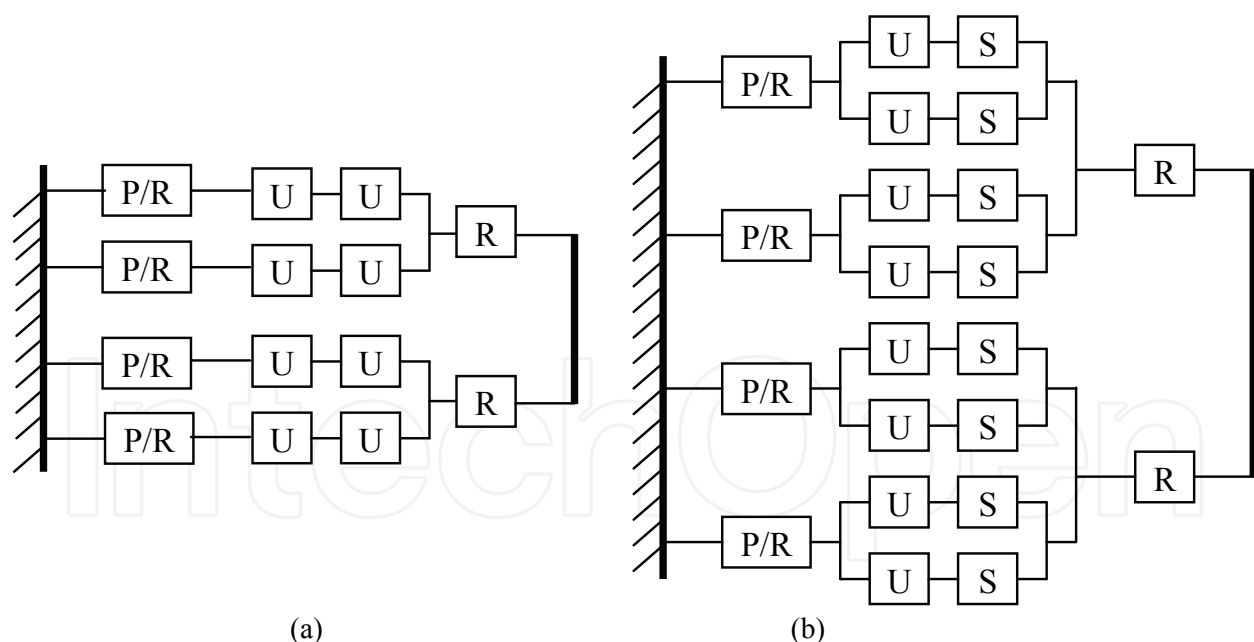


Fig.4. Architecture scheme of H4

The demonstration of “quasi-equivalence” between P-U-U and P-(U-S)₂ is proposed in (Company et al., 2003). The following discusses the possible motion of H4 (Pierrot & Company, 1999; Company & Pierrot, 1999).

Firstly, assume that the two rods of the (U-S)₂ chains are parallel to each other. Fig.5 shows a simple scheme of a possible H4 structure. A_i and B_i are the centers of segments $A_{i1}A_{i2}$ and

$B_{i1}B_{i2}$, respectively. Note $A_{i1}B_{i1}=A_{i2}B_{i2}=A_iB_i$ and $u_i=B_{i1}B_{i2}$. With such notations, the impossible motion for the tip of each P-(U-S)₂ chain is the rotation about: $A_iB_i \times u_i$.

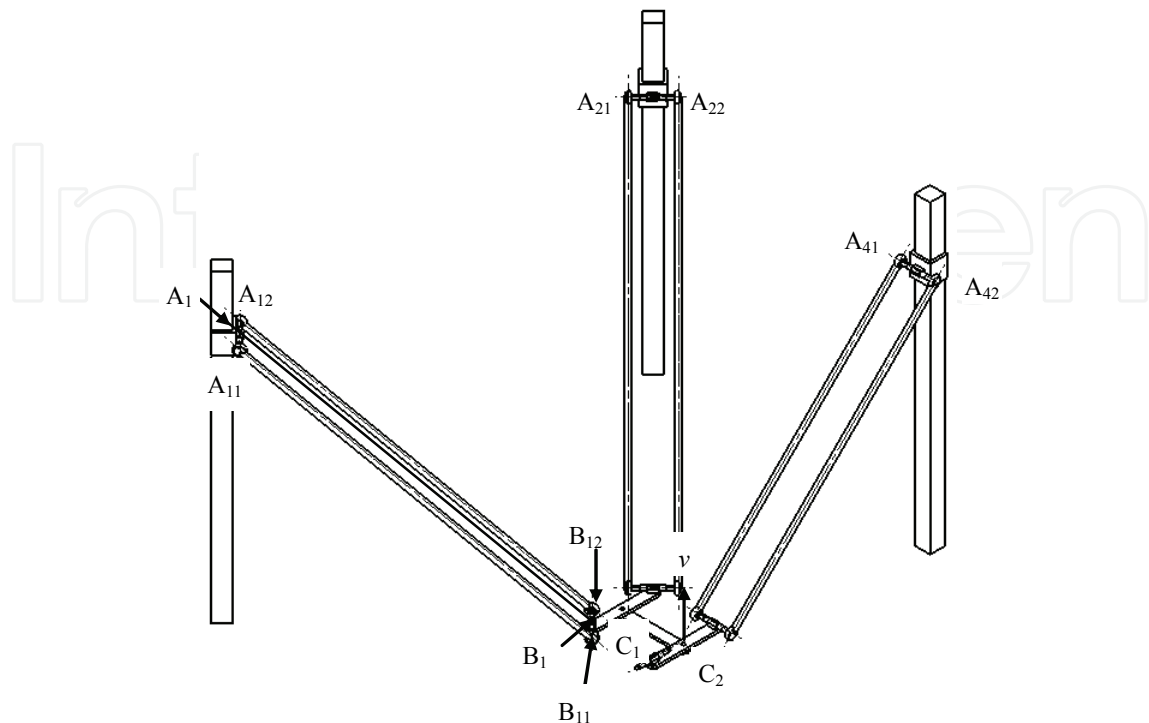


Fig.5 A simple scheme of H4 structure

The link B_1B_2 is connected to the ground by P-(U-S)₂ chains. Each chain provides 3 translations; thus the link B_1B_2 can undergo the same translations. Moreover B_1B_2 cannot rotate about $A_1B_1 \times u_1$, neither about $A_2B_2 \times u_2$ (because the motion that B_1B_2 cannot make is the sum of the impossible motions for each chain). Consequently, B_1B_2 can only rotate about the vector normal to the two previous vectors, namely:

$$(A_1B_1 \times u_1) \times (A_2B_2 \times u_2) \quad (2)$$

The link B_3B_4 has 3 DOFs in translation, and can only rotate about:

$$(A_3B_3 \times u_3) \times (A_4B_4 \times u_4) \quad (3)$$

The link C_1C_2 is connected, on one side, to B_1B_2 by a revolute joint whose direction is represented by vector v_1 , on the other side, to B_3B_4 by a revolute joint whose direction is represented by vector v_2 . Thus, on each side of the nacelle, there are two “meta-chains” which have 5 DOFs. The first chain has 3 translations and 2 rotations about v_1 and $(A_1B_1 \times u_1) \times (A_2B_2 \times u_2)$ respectively. The rotation about $(A_1B_1 \times u_1) \times (A_2B_2 \times u_2) \times v_1$ is impossible. The second “mecha-chain” has 3 translations and 2 rotations about v_2 and $(A_3B_3 \times u_3) \times (A_4B_4 \times u_4)$ respectively. The rotation about $(A_3B_3 \times u_3) \times (A_4B_4 \times u_4) \times v_2$ is impossible. So the possible motions of the nacelle are 3 translations and 1 rotation about $[(A_1B_1 \times u_1) \times (A_2B_2 \times u_2) \times v_1] \times [(A_3B_3 \times u_3) \times (A_4B_4 \times u_4) \times v_2]$. When the two revolute joints

placed on the nacelle have the same direction represented by a unit vector \mathbf{v} , the existence of a rotational motion about \mathbf{v} can be written as follows:

$$\exists \alpha, \quad \alpha \neq 0 \quad [(\mathbf{w}_1 \times \mathbf{w}_2) \times \mathbf{v}] \times [(\mathbf{w}_3 \times \mathbf{w}_4) \times \mathbf{v}] = \alpha \mathbf{v} \quad (4)$$

Where $\mathbf{w}_i = \mathbf{A}_i \mathbf{B}_i \times \mathbf{u}_i$. Equation (4) is equivalent to:

$$\{[(\mathbf{w}_1 \times \mathbf{w}_2) \times \mathbf{v}] \times [(\mathbf{w}_3 \times \mathbf{w}_4) \times \mathbf{v}]\} \cdot \mathbf{v} = \alpha \mathbf{v} \cdot \mathbf{v}$$

Since \mathbf{v} is a unit vector, then we can obtain

$$\{[(\mathbf{w}_1 \times \mathbf{w}_2) \times \mathbf{v}] \times [(\mathbf{w}_3 \times \mathbf{w}_4) \times \mathbf{v}]\} = \alpha \neq 0$$

Thus:

$$(\mathbf{w}_3 \times \mathbf{w}_4) \cdot [(\mathbf{w}_1 \times \mathbf{w}_2) \times \mathbf{v}] = -[(\mathbf{w}_1 \times \mathbf{w}_2) \times (\mathbf{w}_3 \times \mathbf{w}_4)] \cdot \mathbf{v} = \alpha \neq 0$$

So, the necessary condition that the nacelle can rotate about a given axis is:

$$[(\mathbf{w}_1 \times \mathbf{w}_2) \times (\mathbf{w}_3 \times \mathbf{w}_4)] \cdot \mathbf{v} \neq 0 \quad (5)$$

It should be noted that the previous condition is only a necessary condition and any singular configuration is not taken into account. The following should demonstrate that the two rods of the P-(U-S)₂ chain are parallel to each other when the nacelle moves, so the necessary condition (7) is also satisfied.

The rods of the P-(U-S)₂ chain will stay parallel to each other if both links B₁B₂ and B₃B₄ move only in translation with respect to the ground. As a matter of fact, the possible motions of the nacelle imply that the two pivots fixed on the nacelle along the direction of vector \mathbf{v} will keep this direction. Thus the only possible rotation for B₁B₂ and B₃B₄ is about vector \mathbf{v} . But equation (2) indicates that B₁B₂ can only rotate about $\mathbf{w}_1 \times \mathbf{w}_2$. So, as long as $\mathbf{w}_1 \times \mathbf{w}_2$ and \mathbf{v} are not collinear, the link B₁B₂ has no possible rotation. A similar remark can be made for B₃B₄, leading to the two following conditions:

$$\begin{aligned} \mathbf{w}_1 \times \mathbf{w}_2 &\neq \mathbf{v} \\ \mathbf{w}_3 \times \mathbf{w}_4 &\neq \mathbf{v} \end{aligned} \quad (6)$$

In conclusion, if conditions (6) are fulfilled, the links B₁B₂ and B₃B₄ move only in translation, and the rods in a pair will stay parallel to each other.

2.1.3 H4 mechanism with symmetrical design

In this chapter, the symmetrical design of H4 refers to the structure scheme based on four identical P-U-U chains or P-(U-S)₂ chains. The four identical chains provide 4×5=20 DOFs. Thus, two additional 1-DOF joints are needed. H4 uses two rotational joints because they are easy to manufacture with good accuracy at low cost. Two types of typical architecture scheme of H4 are shown in Fig.4. Note that the U-U chains can be replaced by (U-S)₂ chains. Moreover, the actuated prismatic joints could be replaced by actuated rotational joints as well. A symmetrical mechanism with prismatic actuators is shown in Fig.6 (a), while an equivalent mechanism with rotational actuators is shown in Fig.6 (b).

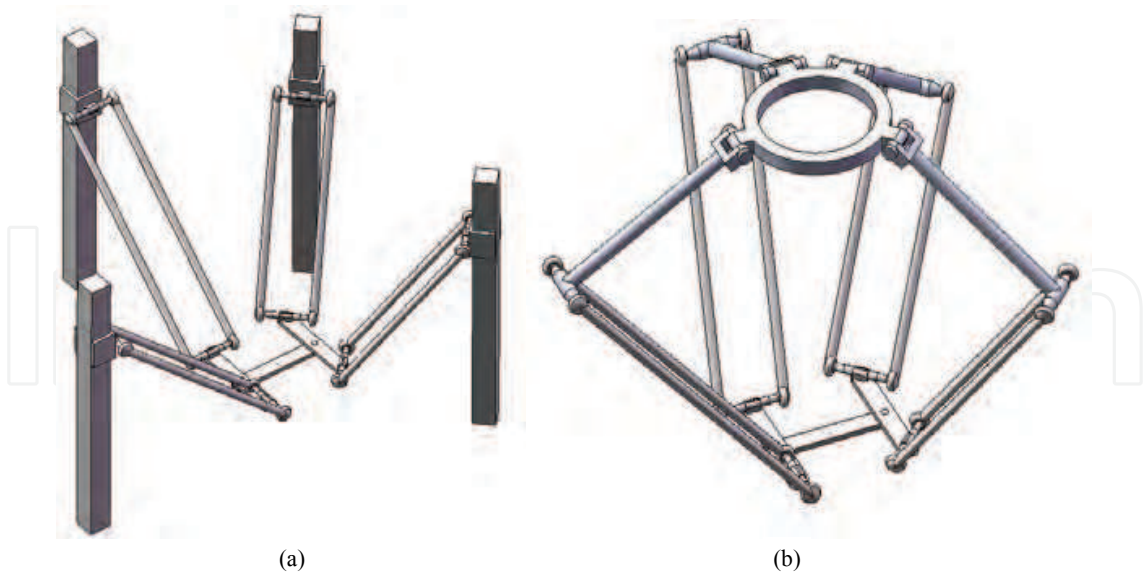


Fig.6. Symmetrical H4 with actuated prismatic joints and rotational joints

2.1.3 H4 mechanism with asymmetrical design

The link B_1B_2 has three translations and a possible rotation about a vector given by equation (2). It is possible to create more advanced mechanisms based on a particular case of equation (2). For example, if $\mathbf{u}_1=\mathbf{u}_2$, then equation (2) becomes:

$$(\mathbf{A}_1\mathbf{B}_1 \times \mathbf{u}_1) \times (\mathbf{A}_2\mathbf{B}_2 \times \mathbf{u}_1) = \beta \mathbf{u}_1$$

As long as $\mathbf{A}_1\mathbf{B}_1 \neq \mathbf{A}_2\mathbf{B}_2$, then $\beta \neq 0$. So the only possible rotation of this link is about vector u_1 . Thus, the first “meta-chain” already fulfilled our requirements: 3 translations and 1 rotation about a given axis. However, this “meta-chain” is only equipped with 2 actuators; thus 2 other chains (with one actuator each) are needed in parallel to lead to a fully-parallel manipulator. If the first “meta-chain” is constituted of two P-U-U chains, it provides $2 \times 5 = 10$ DOFs. So the two additional chains that constitute the second “meta-chain” should be 6

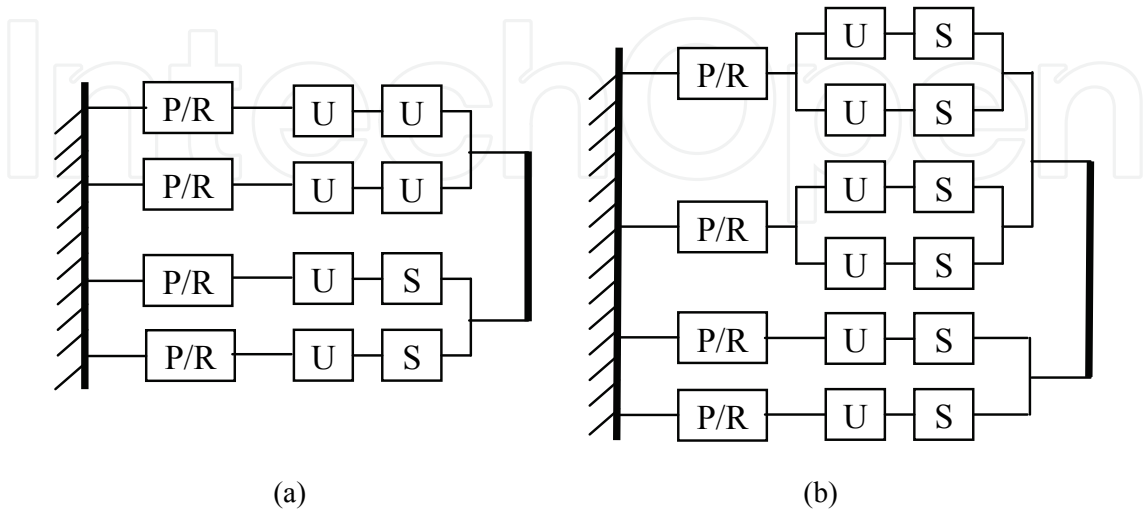


Fig.7 Asymmetrical design of H4

DOFs, which are obviously compatible with the motions offered by the first “meta-chain”. Such mechanical structures are named *asymmetrical H4* (Pierrot & Company, 1999; Company & Pierrot, 1999). An asymmetrical design of H4 using two P-U-Us and two P-U-S's is shown in Fig.7 (a). The P-U-U's can be replaced by P-(U-S)₂'s, as shown in Fig.7 (b).

2.2 Evolution of H4

A new trend in the researches on parallel robotics is the development of lower mobility manipulators. Indeed, a lot of applications do not need six DOFs. A classification proposed by Brogardh (Brogardh, 2002) gives the necessary number of DOF for different industrial applications. He shows that applications such as pick-and-place, assembly, cutting, measurement, etc. just need from three up to five DOFs.

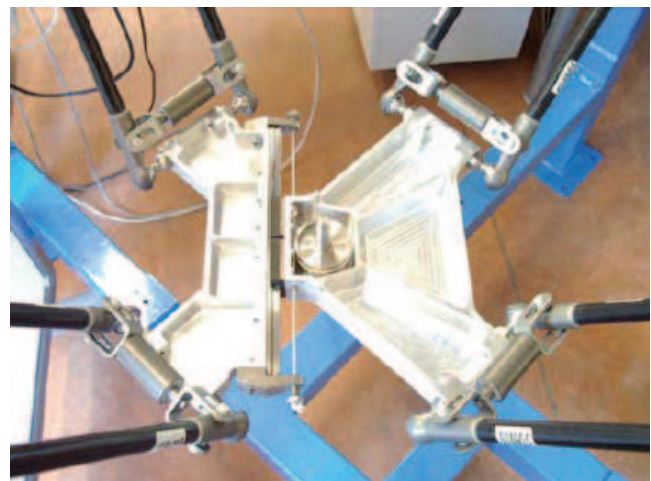
The parallel manipulator H4 can provide three translations and one rotation about a fixed axis, which are also called Schonflies motions (Hervé, 1999). SCARA robots were the first manipulators developed to produce these movements. Due their serial architecture, these robots involve high moving masses which are not suitable for high dynamics. Parallel architecture can overcome this problem. Delta robot is first introduced by Clavel to execute Schonflies motions (Clavel, 1988). This architecture is able to produce three translations and one rotational motion is obtained using a central “telescopic” leg built with universal and prismatic joints. This RUPUR chain suffers from a short service life, and involves a bad stiffness of the rotation motion. Orthoglide (Chablat, 2002) is another parallel robot that can provide Schonflies motions using linear actuators. Its particularity is to be isotropic at the center of its workspace. The machine tool HITA STT has been proposed to produce Schonflies motions (Thurneysen et al, 2002). The particularity of this architecture is to use additional parts in the traveling plate in order to amplify the rotational motion. Other Schonflies motion generators include Gross Manipulator (Angeles et al., 2000), SMG (Angeles, 2005), Kanuk and Manta (Rolland et al., 1999) robots.

In order to avoid the central telescopic leg of the Delta robot, in 1999, the Montpellier Laboratory of Computer Science, Robotics, and Microelectronics (LIRMM) in French invented the parallel manipulator H4 which used the concept of articulated traveling plate. The rotational movement is obtained using an internal mobility on the traveling plate, and a transforming device gives the desired range of rotational motion. Because placing actuators in a symmetrical way (*i.e.* at 90° one relatively to each other) involves “internal singularities” (Pierrot & Company, 1999), the robot has to be built using a particular arrangement of motors. This non-symmetrical arrangement entails a non-homogeneous behavior in the workspace and a limited stiffness of the robot (Company et al., 2005). Later, based on the concept of H4, an improved mechanical structure called I4 is proposed by LIRMM (Krut et al., 2004; Krut et al., 2003). The internal mobility of I4 is obtained with a prismatic joint (Fig. 8). The advantage of this architecture is to authorize a symmetrical arrangement of the actuators. As demonstrates by Krut (Krut et al., 2004), it is possible to place the actuators at 90° one relatively to each other. However, this architecture is more adapted to machine-tool application than to high speed pick-and-place. Indeed, commercial prismatic joints are not suitable for high speed and high accelerations, and have a short service life under such conditions. This inconvenient is due to the high pressure exerted on the balls of these elements at high acceleration conditions. Based on H4 and I4 architecture, an evolution of these mechanisms, named Part 4, has been developed with the wish of reaching high speeds

and accelerations (Nabat et al., 2005). A paper written by Nabat (Nabat et al., 2006) presented experimental results showing that Part 4 was able to reach an acceleration of 15G. Part 4 is a parallel manipulator composed of four closed kinematic chains and an articulated traveling plate. The kinematic chains are similar for Delta, H4 and I4, each of which is composed of an arm and a spatial parallelogram (forearm) linked with spherical joints. The traveling plate is composed of four parts: two main parts (1, 2) linked by two bars (3, 4) with revolute joints (see Fig.9). Thus, its shape is a planar parallelogram and the internal mobility of this traveling plate is a circular translation. Generally, the “natural” range of the rotational operational motion is small, in order to make a complete turn: $[-\pi; \pi]$, an amplification system has to be added on the traveling plate. Several options are available for this amplification such as gears or belt/pulleys. The prototype shown in Fig.9 (b) has been built using belt/pulleys system, with the first pulley fixed on one half traveling plate, and the second one is linked with a revolute joint to the second half traveling plate. Due to its traveling plate having the shape of a planar parallelogram, Part 4 has all the advantages of the previous robots, without their drawbacks. The traveling plate of this robot is articulated and is exclusively realized with revolute joints. Nabat (Nabat et al., 2006) has demonstrated that it is possible to have the same arrangements of the actuators as I4. Thus, this robot is well suited to reach high dynamics and, at the same time, to have a good stiffness and a homogenous behavior in the workspace.



(a) Overview of I4 prototype



(b) Articulated traveling plate

Fig.8. I4 prototype (courtesy of LIRMM)

The use of base-mounted actuators and low-mass links allows the traveling plate to achieve great accelerations. This makes this type of parallel manipulator a perfect candidate for pick and place operations of light objects. Especially for semiconductor end-package equipments, which need high-speed and high-precision pick-and-place movement, these parallel manipulators provide a novel solution scheme.

In this chapter, only H4 is considered, because it firstly provides the most important concept of traveling plate. Based on the analytical method of H4, other types of evolution structure can be analyzed conveniently.

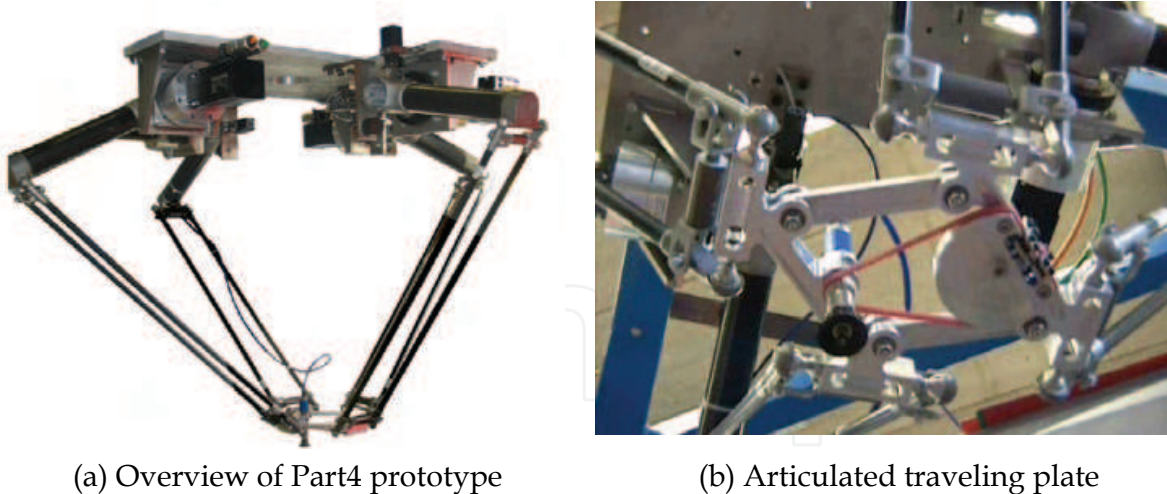


Fig.9. Part4 prototype (courtesy of LIRMM)

3. Kinematic analysis

This section will examine the relations between the actuated joint coordinates of H4 and the nacelle (or traveling plate) pose.

3.1 Inverse kinematics

The relation giving the actuated joint coordinates for a given pose of the end-effector is called the *inverse kinematics*, which is simple for parallel robots. The inverse kinematics consists in establishing the value of the joint coordinates corresponding to the end-effector configuration. Establishing the inverse kinematics is essential for the position control of parallel robots. There are multiple ways to represent the pose of a rigid body through a set of parameters \mathbf{X} . The most classical way is to use the coordinates in a reference frame of a given point C of the body, and three angles to represent its orientation. But there are other ways such as *kinematic mapping* which maps the displacement to a 6-dimensional hyperquadric, the *Study quadric*, in a seventh-dimensional projective space. The kinematic mapping may have an interest as equations involving displacement are algebraic (and the structure of algebraic varieties is better understood than other non-linear structures) and may have interesting properties, for example, stating that a point submitted to a displacement has to lie on a given sphere is easily written as a quadric equation using Study coordinates (Merlet, 2006).

3.1.1 Analytic method

For a fully-parallel mechanism, each of the chains link the base to the moving platform. If \mathbf{A} represents the end of the chain that is linked to the base, and \mathbf{B} the end of the chain that is linked to the moving platform. By construction the coordinates of \mathbf{A} are known in a fixed reference frame, while the coordinates of \mathbf{B} may be determined from the moving platform position and orientation. Hence the vector \mathbf{AB} is fundamental data for the inverse kinematic problem, this is why it plays a crucial role in the solution.

In order to write the position relationship of H4, consider the robotic structure (see Fig.10, chain #4 is not plotted for sake of simplicity). The geometrical parameters of the manipulator at hand are defined as follows:

- Two frames are defined, namely $\{A\}$: a reference frame fixed on the base; $\{B\}$: a coordinate frame fixed on the nacelle (C_1C_2);
- The actuators slide along guide-ways oriented along a unitary vector, \mathbf{k}_z (\mathbf{k}_z is the unity vector along z axis in the reference frame $\{A\}$), and the origin is the point \mathbf{P}_i , so the position of each point \mathbf{A}_i is given by: $\mathbf{A}_i = \mathbf{P}_i + q_i \mathbf{z}_i$, q_i is the moving distance of the actuator. The number $i = 1, 2, 3, 4$ represents each pair of kinematic chains;
- The parameters M_i, d and h are the length of the rods, the offset of the revolute-joint from the ball-joint, and the offset of each ball-joint from the center of traveling plate, respectively;
- The position of the end-effector, namely point \mathbf{B} , is defined by a position vector $\mathbf{B} = [x \ y \ z]$, and a scalar θ , representing the orientation angle.

Without losing generality, in this section we consider $\mathbf{P}_i = (a_i, b_i, 0)$ for simplicity, Q_z is the offset of $\{A\}$ from $\{B\}$ along the direction of \mathbf{k}_z .

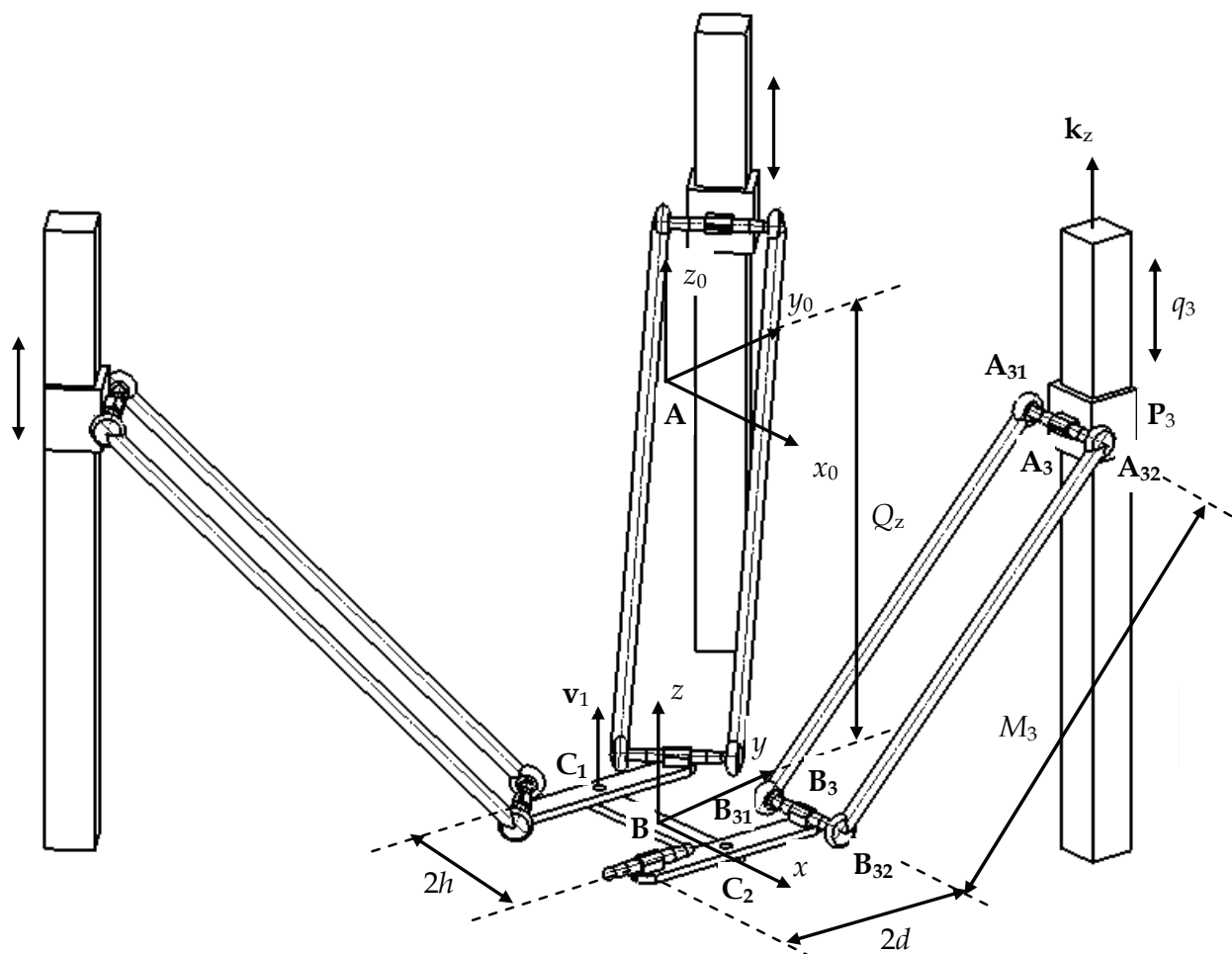


Fig.10. H4 manipulator with four lines drives and $(S-S)_2$ chains

The position of points C_1 and C_2 are given by:

$$\mathbf{C}_1 = \mathbf{B} + \text{Rot}(\mathbf{v}, \theta)(\mathbf{BC}_1) \quad \mathbf{C}_2 = \mathbf{B} + \text{Rot}(\mathbf{v}, \theta)(\mathbf{BC}_2) \quad (7)$$

Where $Rot(\mathbf{v}, \theta)$ denotes the rotation matrix of nacelle with respect to reference frame. The position of each point B_i is given by:

$$\begin{aligned} \mathbf{B}_1 &= \mathbf{C}_1 + \mathbf{C}_1 \mathbf{B}_1 & \mathbf{B}_2 &= \mathbf{C}_1 + \mathbf{C}_1 \mathbf{B}_2 \\ \mathbf{B}_3 &= \mathbf{C}_2 + \mathbf{C}_2 \mathbf{B}_3 & \mathbf{B}_4 &= \mathbf{C}_2 + \mathbf{C}_2 \mathbf{B}_4 \end{aligned} \quad (8)$$

The position relationship can then be written as:

$$\|\mathbf{A}_i \mathbf{B}_i\|^2 = M_i^2 \quad (9)$$

Then for the first axis:

$$\begin{aligned} \mathbf{A}_1 \mathbf{B}_1 &= [\mathbf{B} + Rot(\mathbf{v}, \theta)(\mathbf{BC}_1) + \mathbf{C}_1 \mathbf{B}_1 - \mathbf{P}_1] - q_1 \mathbf{z}_1 \\ (\mathbf{A}_1 \mathbf{B}_1)^2 &= q_1^2 - 2q_1 \mathbf{d}_1 \cdot \mathbf{z}_1 + \mathbf{d}_1^2 \end{aligned} \quad (10)$$

where $\mathbf{d}_1 = \mathbf{B} + Rot(\mathbf{v}, \theta)(\mathbf{BC}_1) + \mathbf{C}_1 \mathbf{B}_1 - \mathbf{P}_1$. Finally, the two solutions are given by:

$$q_1 = \mathbf{d}_1 \cdot \mathbf{z}_1 \pm \sqrt{(\mathbf{d}_1 \cdot \mathbf{z}_1)^2 + M_1^2 - \mathbf{d}_1^2} \quad (11)$$

Similar derivations give the solution for q_2 , q_3 and q_4 .

3.1.2 Geometrical method

The geometrical approach to the inverse kinematics problem is to consider that the extremities A , B of each chain have a known position in 3D space. The leg can be cut at a point M and two different mechanisms M_A , M_B constituted of the chain between A , M and the chain between B , M can be gotten. The free motion of the joints in these two chains will be such that point M , considered as a member of M_A , will lie on a variety V_A , while considered as a member of M_B it will lie on a variety V_B . If assume the mechanism have only classical lower pairs, these varieties will be algebraic with dimensions d_A , d_B . In the 3D space, a variety of dimension d is defined through a set of $3-d$ independent equations, and hence V_A , V_B will be defined by $3-d_A$ and $3-d_B$ equations. The solutions of the inverse kinematic problem lie at the intersection of these varieties. As the number of solutions must be finite (otherwise the robot cannot be controlled), the rank of the intersection variety must be 0. In other words, in order to determine the 3 coordinates of the points, $3-d_A+3-d_B$ should equal to 3 or d_A+d_B equal to 3 (Merlet, 2006).

The key problem about the geometrical method rests with the choice of the cutting point. For the H4 structure shown in Fig.10, B_i are chosen as the cutting points. Points B_i has to lie on a sphere centered at A_i with radius M_i , while for the nacelle, the coordinates of Points B_i can be described as (8). Hence to obtain the intersection of these 2 varieties the known distance between A , B of should be equal to M_i : this equation will give the joint coordinates q_i . The same results can be obtained as described as (11).

3.2 Direct kinematics

Direct kinematics addresses the problem of determining the pose of the end-effector of a parallel manipulator from its actuated joint coordinates. This relation has a clear practical interest for the control of the pose of the manipulator, but also for the velocity control of the end-effector.

In general, the solutions for determining the pose of the end-effector from measurements of the minimal set of joint coordinates that are necessary for control purposes is not unique. There are several ways of assembling a parallel manipulator with given actuated joint coordinates, and generally the direct kinematic relationship cannot be expressed in an analytical manner. Although various methods have been presented for finding all the solutions for this problem and their computation times are decreasing (Faugère, 1995; Hesselbach & Kerle, 1995; Gosselin, 1996; Merlet, 2004), it is still difficult to use these algorithms in a real time context. Furthermore, there is no known algorithm that allows the determination of the current pose of the platform among the set of solutions. The numerical methods using a-priori information on the current pose are more compatible with a real-time context, while their convergence and robustness is an important issue. As direct kinematics is an important issue for control, it may be necessary and interesting to investigate how to improve the computation time. Besides the progress in algorithms and processor speed, one possible approach to solve these problem is to add sensors (i.e. to have more than n sensors for a n -DOF manipulator) to obtain information, allowing a faster calculation of the current pose of the platform, at the cost of more complex hardware (Bonev et al., 2001; Chui & Perng; 2001; Parenti-Castelli, 2001). Merlet has pointed out several unsolved problems about the parallel robot's direct kinematics (Merlet, 2000). Especially the *algebraic geometry* and *computational kinematics* should bring about enough attention.

The first step of solving direct kinematics is to determine a bound on its maximal number of solution. Then, the equations are reduced for the system to obtain the solution of a univariate polynomial whose degree should be determined in the previous analysis. Many researchers have tried to obtained closed-form solutions of parallel robots in a univariate polynomial equation. Especially, the 3- and 6- DOFs parallel robots, e.g., planar, Delta, Steward platform and Hexapod robots, have been mainly considered. This section provides a univariate polynomial equation for H4. It is shown that the solutions of the forward kinematics yield a 16th degree polynomial in a single variable (Choi et al., 2003).

3.2.1 Forward kinematics formulation

The forward kinematics of the H4 is the problem of computing the position and orientation of the nacelle (traveling plate) from the motor angles or the moving distance of the actuator. To get a closed-form solution, a univariate polynomial equation needs to be solved. The following method is extracted from the paper written by Choi (Choi et al., 2003).

The kinematic structure of H4 is shown in Fig.10 and design parameters are shown in Fig.11. The nacelle is composed of three parts (two lateral bars and one central bar). The four points B_1 , B_2 , B_3 and B_4 form a parallelogram. Let ${}^A B_i$ and ${}^A A_i$ represent the homogeneous coordinates of the points B_i in $\{A\}$ and A_i in $\{A\}$ respectively. Then the homogeneous coordinates of ${}^A B_i$ and ${}^A A_i$ can be written as:

$${}^A B_i = \begin{bmatrix} x + hE_{1i} \cos \theta \\ y + hE_{1i} \sin \theta + dE_{2i} \\ z \\ 1 \end{bmatrix} = \begin{bmatrix} P_i i_x + x \\ P_i i_y + y + Q_i \\ z \\ 1 \end{bmatrix} \quad (12)$$

$${}^A A_i = [a_i \quad b_i \quad q_i \quad 1]^T$$

where
 $i_x = \cos \theta$, $i_y = \sin \theta$, $P_i = hE_{1i}$, $Q_i = dE_{2i}$, $E_{11} = E_{12} = -1$, $E_{13} = E_{14} = 1$, $E_{21} = E_{24} = -1$,
 $E_{22} = E_{23} = 1$.

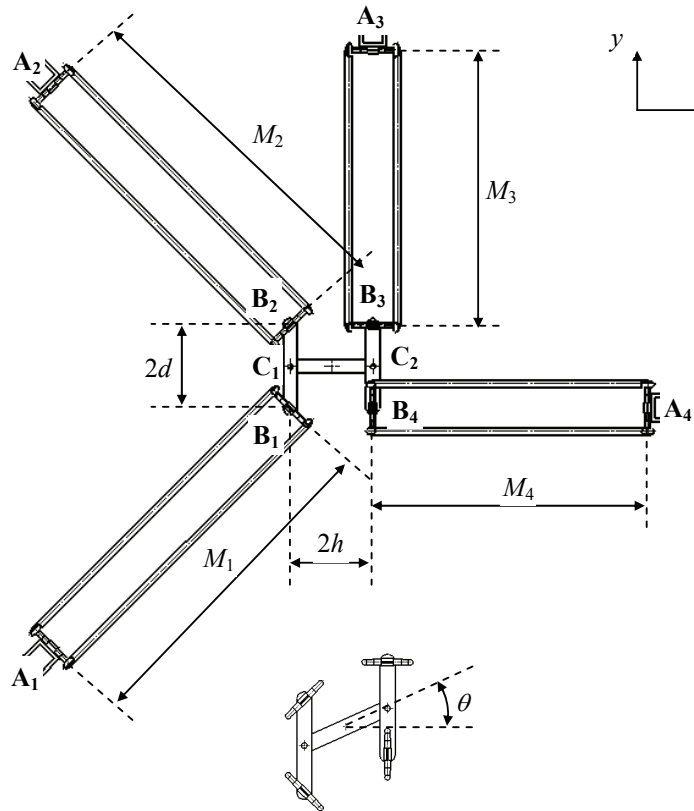


Fig.11. Design parameters of H4

The kinematic closure of each elementary chain can be written as:

$$\left\| {}^A \mathbf{A}_i {}^A \mathbf{B}_i \right\|^2 = M_i^2 \tag{13}$$

Consequently, the each chain provides us with the following equation:

$$\left(P_i i_x + x - a_i \right)^2 + \left(P_i i_y + y + Q_i - b_i \right)^2 + \left(z - q_i \right)^2 = M_i^2 \tag{14}$$

Expanding and rearranging equation (14), the following equation is obtained:

$$\tilde{A}_i x + \tilde{B}_i y + \tilde{C}_i z + \tilde{D}_i + \tilde{E}_i = 0 \tag{15}$$

where, $\tilde{A}_i = 2(P_i i_x - a_i)$, $\tilde{B}_i = 2(P_i i_y + Q_i - b_i)$, $\tilde{C}_i = -2q_i$,
 $\tilde{D}_i = a_i^2 + b_i^2 + q_i^2 - 2P_i(a_i i_x + b_i i_y - Q_i i_y) - 2Q_i b_i + P_i^2 + Q_i^2 - M_i^2$, $\tilde{E}_i = x^2 + y^2 + z^2$

From equation (15), the four equations become:

$$\tilde{A}_1 x + \tilde{B}_1 y + \tilde{C}_1 z + \tilde{D}_1 + \tilde{E}_1 = 0 \tag{16}$$

$$\tilde{A}_2x + \tilde{B}_2y + \tilde{C}_2z + \tilde{D}_2 + \tilde{E}_2 = 0 \quad (17)$$

$$\tilde{A}_3x + \tilde{B}_3y + \tilde{C}_3z + \tilde{D}_3 + \tilde{E}_3 = 0 \quad (18)$$

$$\tilde{A}_4x + \tilde{B}_4y + \tilde{C}_4z + \tilde{D}_4 + \tilde{E}_4 = 0 \quad (19)$$

Choosing any three from the above four equations, we can eliminate x^2 , y^2 and z^2 simultaneously and obtain an equation with variables x , y and z . Subtracting equation (18) from equation (17) and equation (19) from equation (17) respectively, the following two equations are obtained, which are used to eliminate x and y to obtain a polynomial in a single variable z .

$$\Delta A_{23}x + \Delta B_{23}y + \Delta C_{23}z + \Delta D_{23} = 0 \quad (20)$$

$$\Delta A_{24}x + \Delta B_{24}y + \Delta C_{24}z + \Delta D_{24} = 0 \quad (21)$$

where, $\Delta A_{23} = (\tilde{A}_2 - \tilde{A}_3)$, $\Delta B_{23} = (\tilde{B}_2 - \tilde{B}_3)$, $\Delta C_{23} = (\tilde{C}_2 - \tilde{C}_3)$, $\Delta D_{23} = (\tilde{D}_2 - \tilde{D}_3)$, $\Delta A_{24} = (\tilde{A}_2 - \tilde{A}_4)$, $\Delta B_{24} = (\tilde{B}_2 - \tilde{B}_4)$, $\Delta C_{24} = (\tilde{C}_2 - \tilde{C}_4)$, $\Delta D_{24} = (\tilde{D}_2 - \tilde{D}_4)$.

From equation (20) and (21), x and y are solved as:

$$x = \frac{\Delta_{11}z + \Delta_{12}}{\Delta_0} = e_1z + e_2 \quad (22)$$

$$y = \frac{\Delta_{21}z + \Delta_{22}}{\Delta_0} = e_3z + e_4 \quad (23)$$

where, $e_1 = \frac{\Delta_{11}}{\Delta_0}$, $e_2 = \frac{\Delta_{12}}{\Delta_0}$, $e_3 = \frac{\Delta_{21}}{\Delta_0}$, $e_4 = \frac{\Delta_{22}}{\Delta_0}$, with $\Delta_0 = \Delta A_{23}\Delta B_{24} - \Delta A_{24}\Delta B_{23}$,

$\Delta_{11} = \Delta B_{23}\Delta C_{24} - \Delta B_{24}\Delta C_{23}$, $\Delta_{12} = \Delta B_{23}\Delta D_{24} - \Delta B_{24}\Delta D_{23}$, $\Delta_{21} = \Delta A_{24}\Delta C_{23} - \Delta A_{23}\Delta C_{24}$, $\Delta_{22} = \Delta A_{24}\Delta D_{23} - \Delta A_{23}\Delta D_{24}$.

Substituting equations (22) and (23) into equation (17), the following quadratic equation is obtained:

$$\lambda_0z^2 + \lambda_1z + \lambda_2 = 0 \quad (24)$$

where, $\lambda_0 = e_1^2 + e_3^2 + 1$, $\lambda_1 = 2e_1e_2 + 2e_3e_4 + \tilde{A}_2e_1 + \tilde{B}_2e_3 + \tilde{C}_2$, $\lambda_2 = e_2^2 + e_4^2 + \tilde{A}_2e_2 + \tilde{B}_2e_4 + \tilde{D}_2$.

From equation (24), z can be calculated as:

$$z = \frac{-\lambda_1 + \rho}{2\lambda_0} \quad (25)$$

where,

$$\rho = \pm \sqrt{\lambda_1^2 - 4\lambda_0\lambda_2} \quad (26)$$

Substituting equations (22), (23) and (25) into equation (16), the following equation is obtained:

$$\rho^2 - 2(\lambda_1 - \lambda_1')\rho + \lambda_1^2 - 2\lambda_1\lambda_1' + 4\lambda_0\lambda_2' = 0 \quad (27)$$

where, $\lambda_1' = 2e_1e_2 + 2e_3e_4 + \tilde{A}_1e_1 + \tilde{B}_1e_3 + \tilde{C}_1$, $\lambda_2' = e_2^2 + e_4^2 + \tilde{A}_2e_2 + \tilde{B}_2e_4 + \tilde{D}_1$.

The variable ρ can be calculated from equation (27):

$$\rho = (\lambda_1 - \lambda_1') \pm \sqrt{\lambda_1'^2 - 4\lambda_0\lambda_2'} \quad (28)$$

So the right parts of equations (26) and (28) are equivalent:

$$(\lambda_1 - \lambda'_1) \pm \sqrt{\lambda_1'^2 - 4\lambda_0\lambda'_2} = \pm \sqrt{\lambda_1^2 - 4\lambda_0\lambda_2} \quad (29)$$

By taking the second power of the both sides of equation (29), a polynomial equation with variables i_x and i_v can be obtained as follows:

$$\lambda_0[\Delta\lambda_1 \cdot (\lambda_1\lambda'_2 - \lambda'_1\lambda_2) + \lambda_0 \cdot \Delta\lambda_2^2] = 0 \quad (30)$$

where, $\Delta\lambda_1 = \lambda_1 - \lambda'_1$, $\Delta\lambda_2 = \lambda_2 - \lambda'_2$. Equation (20) can be rewritten as (Choi et al., 2003):

$$f(i_x^8, i_x^7, i_x^7 i_y, i_x^7 i_y, i_x^6, i_x^6 i_y, i_x^6 i_y^2, i_x^5, i_x^5 i_y, i_x^5 i_y^2, i_x^5 i_y^3, i_x^4, i_x^4 i_y, i_x^4 i_y^2, i_x^4 i_y^3, i_x^4 i_y^4, i_x^3, i_x^3 i_y, i_x^3 i_y^2, i_x^3 i_y^3, i_x^3 i_y^4, i_x^3 i_y^5, i_x^2, i_x^2 i_y, i_x^2 i_y^2, i_x^2 i_y^3, i_x^2 i_y^4, i_x^2 i_y^5, i_x^2 i_y^6, i_x, i_x i_y, i_x i_y^2, i_x i_y^3, i_x i_y^4, i_x i_y^5, i_x i_y^6, i_x i_y^0, i_x i_y^0, i_x i_y^0 i_y^2, i_x i_y^0 i_y^3, i_x i_y^0 i_y^4) = 0 \quad (31)$$

where $f(x_1, x_2, \dots, x_n)$ represents a linear combination of x_1, x_2, \dots, x_n . The coefficients of equation (30) are all constant quantities which depend on the geometric parameters of the H4 robot.

Using the following well-known trigonometric function:

$$i_x = \frac{1-T^2}{1+T^2}, i_x = \frac{2T}{1+T^2} \quad (32)$$

where $T = \tan(\theta/2)$, then equation (31) becomes a polynomial equation in a single variable T which contains terms up to the 16th power. This means that the mechanism may have up to 16 different configurations for a given set of actuator's position. Substituting equation (32) into equations (26), (22), (23) and (25), the values of ρ , x , y and z can be gotten respectively.

3.2.2 Numerical example

In this section, a numerical example for the H4 robot shown in Fig.10 and Fig.11 is presented to illustrate the application of the method proposed in the previous section. The design parameters of H4 is chosen as: $h=d=6$, $Q_z=42$, $v=[0 \ 0 \ 1]^T$, $M_1=M_2=\sqrt{3} \ Q_z$, $M_3=M_4=\sqrt{2} \ Q_z$, the origin coordinates of points \mathbf{A}_i and \mathbf{B}_i are set as following:

$$\mathbf{A}_1 = \begin{bmatrix} -48 & -48 & 0 \end{bmatrix}, \mathbf{B}_1 = \begin{bmatrix} -6 & -6 & -42 \end{bmatrix}, \mathbf{A}_2 = \begin{bmatrix} -48 & 48 & 0 \end{bmatrix}, \mathbf{B}_2 = \begin{bmatrix} -6 & 6 & -42 \end{bmatrix},$$

$$\mathbf{A}_3 = \begin{bmatrix} 6 & 48 & 0 \end{bmatrix}, \mathbf{B}_3 = \begin{bmatrix} 6 & 6 & -42 \end{bmatrix}, \mathbf{A}_4 = \begin{bmatrix} 48 & -6 & 0 \end{bmatrix}, \mathbf{B}_4 = \begin{bmatrix} 6 & -6 & -42 \end{bmatrix},$$

$$\mathbf{u} = [\mathbf{u}_1 \quad \mathbf{u}_2 \quad \mathbf{u}_3 \quad \mathbf{u}_4] = \begin{bmatrix} -1 & 1 & 1 & 0 \\ 1 & 1 & 0 & -1 \\ 0 & 0 & 0 & 0 \end{bmatrix}, \text{ where } \mathbf{u}_i = \mathbf{B}_{i1} \mathbf{B}_{i2}.$$

When the position and orientation of the nacelle are set $x=5$, $y=-5$, $z=-30$, $\theta=\pi/6(\text{rad})$, four actuators' position which is calculated by inverse kinematics are given by:

$$q_1=13.021, q_2=-7.488, q_3=9.679, q_4=15.770 \quad (33)$$

For the actuators' position given by equation (33), Matlab Symbolic Math Toolbox is used to solve the polynomial equation with variable T . The results indicate that there are only twelve solutions, the author believes that there are several repeated roots. This result needs further study. The two real roots are $T=0.268$ and $T=-2.882$ respectively. When set $T=0.268$, the configuration of the nacelle is calculated as: $x=5\text{mm}$, $y=-5\text{mm}$, $z=-30\text{mm}$, $\theta=0.524(\text{rad})$, which is the expected solutions. When set $T=-2.882$, the configuration of the nacelle is calculated as: $x=3\text{mm}$, $y=-7.95\text{mm}$, $z=-14.58\text{mm}$, $\theta=-2.47(\text{rad})$. This configuration cannot be realized in practice because of the mutual interference of the parallelograms as shown in Fig.11.

3.3 Jacobian matrix

Jacobian matrix relates the actuated joint velocities to the end-effector cartesian velocities, and is essential for the velocity and trajectory control of parallel robots. For parallel manipulators, their inverse Jacobian matrix can be established without a very high complexity, but their Jacobian matrix cannot be obtained directly, even with the help of symbolic computation, except in some particular cases (Bruyninckx, 1997; Pennock & Kassner, 1990). Theoretical analytic formulations of jacobians have been proposed, but require complicated matrix inversions (Dutr   et al., 1997; Kim et al., 2000). Generally, the difficulty of the inversion does not lie in the complexity of the algorithm but in the sheer size of the result (Merlet, 2006).

The velocity of the nacelle can be defined by resorting to a velocity for the translation, $\mathbf{v}_B = [\dot{x} \quad \dot{y} \quad \dot{z}]$ and a scalar for the rotation about \mathbf{v} , $\dot{\theta}$. Thus, the velocity of points C_1 and C_2 can be written as follows (Pierrot & Company, 1999):

$$\mathbf{v}_{C_1} = \mathbf{v}_B + \dot{\theta} \mathbf{v} \times \mathbf{BC}_1 \quad \mathbf{v}_{C_2} = \mathbf{v}_B + \dot{\theta} \mathbf{v} \times \mathbf{BC}_2$$

Moreover, since the links B_1B_2 and B_3B_4 move only in translation, the following relations hold:

$$\mathbf{v}_{B_1} = \mathbf{v}_{B_2} = \mathbf{v}_{C_1} \quad \mathbf{v}_{B_3} = \mathbf{v}_{B_4} = \mathbf{v}_{C_2}$$

On the other hand, velocity of points A_i is given by:

$$\mathbf{v}_{A_i} = \dot{q}_i \mathbf{z}_i$$

where \mathbf{z}_i is the unit vector along the direction of prismatic. The velocity relationship can then be written thanks to the classical property:

$$\mathbf{v}_{A_i} \cdot \mathbf{A}_i \mathbf{B}_i = \mathbf{v}_{B_i} \cdot \mathbf{A}_i \mathbf{B}_i \quad (34)$$

Equation (34) can be written for $i=1, \dots, 4$ and the results grouped in a matrix form, such as:

$$\mathbf{J}_q \dot{\mathbf{q}} = \mathbf{J}_x \dot{\mathbf{x}}$$

where

$$\mathbf{J}_q = \begin{bmatrix} (\mathbf{A}_1 \mathbf{B}_1 \cdot \mathbf{z}_1) & 0 & 0 & 0 \\ 0 & (\mathbf{A}_2 \mathbf{B}_2 \cdot \mathbf{z}_2) & 0 & 0 \\ 0 & 0 & (\mathbf{A}_3 \mathbf{B}_3 \cdot \mathbf{z}_3) & 0 \\ 0 & 0 & 0 & (\mathbf{A}_4 \mathbf{B}_4 \cdot \mathbf{z}_4) \end{bmatrix}$$

$$\dot{\mathbf{q}} = [\dot{q}_1 \quad \dot{q}_2 \quad \dot{q}_3 \quad \dot{q}_4]^T$$

$$\mathbf{J}_x = \begin{bmatrix} (\mathbf{A}_1 \mathbf{B}_1)_x & (\mathbf{A}_1 \mathbf{B}_1)_y & (\mathbf{A}_1 \mathbf{B}_1)_z & (\mathbf{A}_1 \mathbf{B}_1 \times \mathbf{BC}_1) \cdot \mathbf{v} \\ (\mathbf{A}_2 \mathbf{B}_2)_x & (\mathbf{A}_2 \mathbf{B}_2)_y & (\mathbf{A}_2 \mathbf{B}_2)_z & (\mathbf{A}_2 \mathbf{B}_2 \times \mathbf{BC}_1) \cdot \mathbf{v} \\ (\mathbf{A}_3 \mathbf{B}_3)_x & (\mathbf{A}_3 \mathbf{B}_3)_y & (\mathbf{A}_3 \mathbf{B}_3)_z & (\mathbf{A}_3 \mathbf{B}_3 \times \mathbf{BC}_2) \cdot \mathbf{v} \\ (\mathbf{A}_4 \mathbf{B}_4)_x & (\mathbf{A}_4 \mathbf{B}_4)_y & (\mathbf{A}_4 \mathbf{B}_4)_z & (\mathbf{A}_4 \mathbf{B}_4 \times \mathbf{BC}_2) \cdot \mathbf{v} \end{bmatrix}$$

$$\dot{\mathbf{x}} = [\dot{x} \quad \dot{y} \quad \dot{z} \quad \dot{\theta}]$$

If the mechanism is not in a singular configuration, the inverse Jacobian matrix is described as:

$$\mathbf{J}^{-1} = \mathbf{J}_q^{-1} \mathbf{J}_x \quad (35)$$

And the Jacobian matrix is:

$$\mathbf{J} = \mathbf{J}_x^{-1} \mathbf{J}_q \quad (36)$$

When the determinant of inverse Jacobian matrix equals to zero, the parallel manipulator is in a singular configuration, which is a general method for identifying the singular configurations of parallel manipulators. But for a manipulator with $n < 6$ DOF, it should be noted that it may not be efficient to identify all the singular configurations by determining only the $n \times n$ inverse kinematic Jacobian that relates the actuated joint velocities to the possible DOF velocities. Next section will discuss an inverse kinematic Jacobian that involves actuated joints velocities and the full twist of the end-effector, which may be essential for singularity analysis. This type of matrix is coined as *overall jacobian* by Joshi (Joshi & Tsai, 2002), while Merlet called it a *full inverse kinematic jacobian* (Merlet, 2006).

3.4 Determination of the joint velocities and twist

The purpose of this section is to calculate the actuated joint (or end-effector) velocities, being given the end-effector (or actuated joint) velocities.

In the previous section, equation (35) can be applied to compute the actuated joint velocities directly. For example, the structure and design parameters of H4 is described in Fig.10 and

Fig.11, where the following parameters are chosen as described in section 3.2.2. So, according to equation (35), the inverse Jacobian matrix can be expressed as:

$$\mathbf{J}^{-1} = \begin{bmatrix} -1 & -1 & 1 & -6 \\ -1 & 1 & 1 & 6 \\ 0 & 1 & 1 & -6 \\ 1 & 0 & 1 & 0 \end{bmatrix}$$

This inverse Jacobian matrix can be used to calculate the actuated joint velocity directly when the pose of the nacelle is shown in Fig.11.

It is usually difficult, even for robots with less than 6-DOFs robots, to invert \mathbf{J}^{-1} analytically. So a numerical procedure will be needed to calculate the twist of the nacelle from the joint velocities. For a given pose of the end-effector, there are two methods to determine the Jacobian matrix, namely, a numerical inversion algorithm and the quasi-Newton scheme (Reboulet, 1985; Merlet, 2006).

$$\mathbf{J}_{k+1} = \mathbf{J}_k + \mathbf{J}_0(\dot{\mathbf{q}} - \mathbf{J}^{-1}\mathbf{J}_k) \quad (37)$$

where $\dot{\mathbf{q}}$ is the actuated joint velocity; \mathbf{J}_0 denotes the kinematic jacobian matrix calculated for a given pose. The algorithm stops when the differences between the joint velocities and those that are calculated from the twist are lower than a fixed threshold.

For the H4 structure and design parameters described above, when the actuated joint velocities is $\mathbf{q} = [q_1 \ q_2 \ q_3 \ q_4] = [1 \ -1 \ 1 \ 1]$, the speed of the nacelle can reach $\dot{\mathbf{x}} = [\dot{x} \ \dot{y} \ \dot{z} \ \dot{\theta}] = [0.5 \ -0.25 \ 0.5 \ -0.125]$.

3.5 Accelerations analysis

This section will determine what are the relations between the actuated joint accelerations and the cartesian and angular accelerations of the end-effector. H4 presents excellent characteristics as to acceleration which can reach 10g. For parallel robots it is generally easy to obtain these relations directly. From the equation $\dot{\mathbf{q}} = \mathbf{J}^{-1}\dot{\mathbf{x}}$, the following can be obtained by differentiation

$$\ddot{\mathbf{q}} = \mathbf{J}^{-1}\ddot{\mathbf{x}} + \dot{\mathbf{J}}^{-1}\dot{\mathbf{x}} \quad (38)$$

For the various categories of parallel manipulators, the determination of the acceleration equations thus amounts to the determination of the derivative of the inverse kinematic jacobian matrix (Merlet, 2006).

But for H4, the method described above is not intuitionistic. So we derive the relations between the actuated joint accelerations and the accelerations of the end-effector using geometric method. From equation (12), accelerations of the point B_i and A_i in $\{\mathbf{A}\}$ can be obtained as:

$$\begin{aligned} a_{B_i} &= [\ddot{x} - hE_{li} \cos \theta \cdot \ddot{\theta} \quad \ddot{y} - hE_{li} \sin \theta \cdot \ddot{\theta} \quad \ddot{z}]^T \\ a_{A_i} &= [0 \quad 0 \quad \ddot{q}_i]^T \end{aligned} \quad (39)$$

The acceleration projection of points B_i and A_i on the line A_iB_i is equal. So the following equation comes into existence:

$$a_{A_i} \cdot \mathbf{A}_i \mathbf{B}_i = a_{B_i} \cdot \mathbf{A}_i \mathbf{B}_i \quad (40)$$

Equation (40) can be written for $i=1,\dots,4$ and the results grouped in a matrix form, such as:

$$\mathbf{J}_q \ddot{\mathbf{q}} = \mathbf{J}_a \ddot{\mathbf{x}} \quad (41)$$

where

$$\ddot{\mathbf{q}} = [\ddot{q}_1 \quad \ddot{q}_2 \quad \ddot{q}_3 \quad \ddot{q}_4]^T$$

$$\mathbf{J}_a = \begin{bmatrix} (\mathbf{A}_1 \mathbf{B}_1)_x & (\mathbf{A}_1 \mathbf{B}_1)_y & (\mathbf{A}_1 \mathbf{B}_1)_z & -((\mathbf{A}_1 \mathbf{B}_1)_x \cos \theta + (\mathbf{A}_1 \mathbf{B}_1)_y \sin \theta) \cdot hE_{11} \\ (\mathbf{A}_2 \mathbf{B}_2)_x & (\mathbf{A}_2 \mathbf{B}_2)_y & (\mathbf{A}_2 \mathbf{B}_2)_z & -((\mathbf{A}_2 \mathbf{B}_2)_x \cos \theta + (\mathbf{A}_2 \mathbf{B}_2)_y \sin \theta) \cdot hE_{12} \\ (\mathbf{A}_3 \mathbf{B}_3)_x & (\mathbf{A}_3 \mathbf{B}_3)_y & (\mathbf{A}_3 \mathbf{B}_3)_z & -((\mathbf{A}_3 \mathbf{B}_3)_x \cos \theta + (\mathbf{A}_3 \mathbf{B}_3)_y \sin \theta) \cdot hE_{13} \\ (\mathbf{A}_4 \mathbf{B}_4)_x & (\mathbf{A}_4 \mathbf{B}_4)_y & (\mathbf{A}_4 \mathbf{B}_4)_z & -((\mathbf{A}_4 \mathbf{B}_4)_x \cos \theta + (\mathbf{A}_4 \mathbf{B}_4)_y \sin \theta) \cdot hE_{14} \end{bmatrix}$$

$$\ddot{\mathbf{x}} = [\ddot{x} \quad \ddot{y} \quad \ddot{z} \quad \ddot{\theta}]$$

For the H4 structure and design parameters described above, when the nacelle is in the origin pose and the actuated joint accelerations are $\ddot{\mathbf{q}} = [10 \quad -10 \quad 10 \quad 10] \text{m/s}^2$, the linear acceleration of the nacelle can reach 23m/s^2 and the angular acceleration can reach 2.5rad/s^2 .

3.6 Kinetostatic performance indices

3.6.1 Manipulability

The inverse kinematic jacobian matrix reflects a linear relation between the manipulator accuracy $\Delta \mathbf{x}$ and the measurement errors $\Delta \mathbf{q}$ on \mathbf{q} . If the measurement errors are bounded, then the hyper-sphere in the joint error space can be mapped into an ellipsoid in the generalized Cartesian error space with using the Euclidean norm. This ellipsoid is usually called the *manipulability ellipsoid*. If using the infinity norm, the joint errors are restricted to lie in a hyper-cube in the joint error space. The hyper-cube in the joint error space can be mapped into the *kinematic polyhedron* in the positioning errors space (Merlet, 2006). The shape and volume of the manipulability ellipsoid and the kinematic polyhedron characterize the manipulator dexterity. It is necessary to set up some kinetostatic performance indices that are used to quantify the dexterity of a robot. The famous Yoshikawa's *manipularity index* $\sqrt{\mathbf{J} \mathbf{J}^T}$ is used for serial robots for a long time. Another index is the *condition number* that is often used for parallel robots.

$$\kappa = \|\mathbf{J}^{-1}\| \|\mathbf{J}\| \quad (42)$$

The condition number expresses how a relative error in joint space gets multiplied and leads to a relative error in work space. The condition number is dependent on the choice of the metric norm and the most used norms are the 2-norm and the Euclidean norm. The condition number is mentioned as the main index for characterizing the accuracy of parallel robots. But there is major drawback to the condition number for H4, since the elements of the matrix corresponding to translations are dimensionless, whereas those corresponding to the rotations are lengths. A direct consequence is that the condition number has no clear

physical meaning, as the rotations are transformed arbitrarily into “equivalent” translations (Merlet, 2006). There are various proposals that have been made to avoid this drawback (Gosselin, 1990; Kim & Ryu, 2003). But all these proposals have their own special drawbacks. How to design a general law for parallel robots’ manipulability is still an open problem.

3.6.2 Isotropy

Poses with a condition number of 1 are called *isotropic poses*, and robots having only such type of poses are called isotropic robots (Merlet, 2006). At the given pose as shown in Fig.11, the condition number of H4 is about 8.56 and there is no any isotropic poses in the workspace of H4 (Company et al., 2005). While Part4 robots which are the evolutionary structure of H4 are isotropic at their original poses.

There are some other manipulability and accuracy indices, such as global conditioning index, uniformity of manipulability and maximal positioning error index et al. All the above definitions of the kinetostatic indices do not take into account other factor affecting the accuracy of parallel robots, such as manufacturing tolerances, clearance and friction in the joints. In order to include these factors in accuracy analysis, Monte Carlo statistical simulation technique can be used to evaluate the accuracy of parallel manipulators (Ryu & Cha, 2003).

4. Singularity analysis

This section will identify all the singular configurations of the H4 and analyze the manipulator’s self-motion when in or closed to a singular configuration. Generally, singular configurations refer to particular poses of the end-effector, for which parallel robots lose their inherent infinite rigidity, and in which the end-effector will have uncontrollable degrees of freedom. But for this new family of parallel manipulator H4, singularities are associated with either loss or gain of DOF. This section utilizes line geometry tools and screw theory to deal with singularity analysis of H4. Firstly, the basic theory including in the process of singularity analysis is introduced briefly. Then the static equilibrium condition of the end-effector is derived to obtain the *full inverse kinematic jacobian* 6×6 matrix, which is set of governing lines of the manipulator. Based on linear dependency of these lines, the singular configurations of the manipulator can be identified. Moreover, in order to deal with singularities associated with loss of DOFs (serial singularity), the static equilibrium of the actuators is also defined. Secondly, architecture and constraint singularities associated with gain of DOFs (parallel singularity) are defined and analyzed using linear complex approximation algorithm (LCAA), which is employed to obtain the closest linear complex, presented by its screw coordinates, to the set of governing lines. The linear complex axis and pitch provide additional information and a better physical understanding of the manipulator’s self-motion when in or closed to a singular configuration. Lastly, various singularities of an example H4 manipulator are presented and analyzed using the proposed methods (Wu et al., 2006).

4.1 Basic theory

In the context of designing a parallel manipulator, understanding the intrinsic nature of singularities and their relations with the kinematic parameters and the configuration spaces

is of great importance. The phenomena of singularity in parallel manipulators have been approached from different points of view. One way to introduce singular configurations is to examine the relations obtained for inverse kinematics. Singularities correspond to the roots of the parallel manipulator Jacobian's determinant. Based on the rank deficiency associated with the Jacobian matrices, singularities of parallel manipulators have been explained (Gosselin & Angeles, 1990; Zlatanov et al., 1994). Using the linear decomposition method and co-factor expansion, St-Onge and Gosselin (St-Onge & Gosselin, 2000) studied the singularity loci of the Gough-Stewart platform, and obtained a graphical representation of these loci in the manipulator workspace. Due to the complexity of the kinematic model, several authors proposed numerical methods to analyze the singularities (Feng-Cheng & Haug, 1994; Funabashi & Takeda, 1995). However, even with symbolic computation software, the calculation of the determinant of Jacobian matrix is a complicated task. Moreover, identifying kinematic singularity through matrices does not provide physical insight into the nature of singular configuration of parallel manipulators.

A parallel manipulator is naturally associated with a set of constraint functions defined by its closure constraints (geometric relations of the closed-chain mechanism). The differential forms arising from these constraint functions completely characterize the geometric properties of the manipulator. So Liu et al. (Liu et al., 2003) used differential geometric tools to study singularities of parallel mechanisms and provided a finer classification of singularities. In their works, they classified singularity into configuration space singularities and parametrization singularities which include actuator and end-effector singularities as their special cases. But the method is too abstract and complicated when dealing with singularities of spatial parallel manipulators.

Another approach to analyze the parallel manipulators' singularity is based on line geometry and screw theory. Merlet (Merlet, 1992) considered the Jacobian matrix of the Gough-Stewart platform as the Plücker line coordinates of the robot's actuators and identified the singular configurations of the robot. In (Romdhane et al., 2002), a mixed geometric and vector formulation is used to investigate the singularities of a 3-translational-DOF parallel manipulator. In (Collins, 1995), singularities of an in-parallel hand controller for force-reflected teleoperation were analyzed, the six columns of the Jacobian matrix were viewed as zero-pitch wrenches (lines) acting on the top platform, then line geometry and rank determining geometric constructions were used to obtain all configuration singularities. Basu and Ghosal (Basu & Ghosal, 1997) presented a geometric condition to deal with the singularity analysis associated with gain of DOF in a class of platform-type, multi-loop spatial manipulators. Joshi and Tsai (Joshi & Tsai, 2002) developed a methodology for the Jacobian analysis of limited-DOF parallel manipulators by making use of the theory of reciprocal screws. A 6×6 Jacobian matrix so derived provided information about both architecture and constraint singularities.

The present investigation identifies all the singular configurations of the H4 robot and provides physical insight into the nature of these singular configurations from the view point of geometry. Moreover, the behavior in these singular configurations or in the neighboring ones is also determined using linear complex approximation. All these analyses need some basic theories, include Grassmann geometry, Line geometry and Screw theory etc. The following gives a brief presentation of these theories.

4.1.1 Line geometry and Plücker coordinates

Line geometry investigates the set of lines in three-space. The ambient space can be a real projective, affine, Euclidean or a non-Euclidean space. Line geometry possesses a close relation to spatial kinematics (Bottema & Roth, 1990) and has therefore found applications in mechanism design and robot kinematics. A parallel manipulator has a singular position if the axes of its hydraulic cylindrical legs lie in a linear complex, a special three-parameter set of lines. In practice, several sources for errors (manufacturing, material properties, computing, etc.) can hardly be avoided. Thus, the question is whether the lines on the objects near their realization are close – within some tolerance – to the lines of a linear complex. This is an approximation or regression problem in line space (Helmut et al., 1999). In real Euclidean space E^3 , a Cartesian coordinate system is used and the points are represented by their coordinate vectors \mathbf{M} . A straight line L can be determined by a point $\mathbf{p} \in L$ and a normalized direction vector \mathbf{l} of L , i.e. $\|\mathbf{l}\| = 1$. To obtain coordinates for L , one forms the moment vector

$$\bar{\mathbf{l}} := \mathbf{p} \times \mathbf{l} \quad (43)$$

with respect to the origin. If \mathbf{p} is substituted by any point $\mathbf{q} = \mathbf{p} + \lambda \mathbf{l}$ on L , equation (43) implies that $\bar{\mathbf{l}}$ is independent of \mathbf{p} on L . The six coordinates $(\mathbf{l}, \bar{\mathbf{l}})$ with

$$\mathbf{l} = (l_1, l_2, l_3), \text{ and } \bar{\mathbf{l}} = (l_4, l_5, l_6)$$

are called the *normalized Plücker coordinates* of L . The set of lines in E^3 is a four-dimensional manifold and accordingly the six Plücker coordinates satisfy two relations. One is the normalization and the other is, by equation (43), the so-called *Plücker relation*

$$\mathbf{l} \cdot \bar{\mathbf{l}} = 0 \quad (44)$$

which expresses the orthogonality between \mathbf{l} and $\bar{\mathbf{l}}$. Conversely, any six-tuple $(\mathbf{l}, \bar{\mathbf{l}})$ with $\|\mathbf{l}\| = 1$, which satisfies the Plücker relation $\mathbf{l} \cdot \bar{\mathbf{l}} = 0$ represents a line in E^3 . As the orientation are not concerned, $(\mathbf{l}, \bar{\mathbf{l}})$ and $(-\mathbf{l}, -\bar{\mathbf{l}})$ describe the same line L .

The topic about the Klein mapping and special sets of lines can refer to the paper written by Pottmann et al. (Pottmann et al., 1999).

4.1.2 Grassmann geometry

As shown in the previous section, two lines with Plücker coordinates $\mathbf{l}_1 = [\mathbf{p}_1, \mathbf{q}_1]$, $\mathbf{l}_2 = [\mathbf{p}_2, \mathbf{q}_2]$ intersect if and only if $\mathbf{p}_1 \cdot \mathbf{q}_1 + \mathbf{q}_2 \cdot \mathbf{p}_2 = 0$. Plücker vectors with $\mathbf{p} = 0$ do not represent real lines and are associated with a line at infinity. All lines at infinity belong to a plane, the plane at infinity. A point may also be represented by the Plücker coordinates (α, \mathbf{r}) so that its coordinates are \mathbf{r}/α . If $\alpha=0$, then the point is at infinity, and a point $(0, \mathbf{r})$ at infinity is on the line at infinity $(0, \mathbf{q})$ if and only if $\mathbf{r} \cdot \mathbf{q} = 0$. Consequently a point at infinity that belongs to the two lines at infinity $(0, \mathbf{s}_1)$, $(0, \mathbf{s}_2)$ has coordinates $(0, \mathbf{s}_1 \times \mathbf{s}_2)$.

The columns of the full inverse kinematic jacobian matrices of most parallel robots are constructed from the Plücker vectors of lines associated with links of the manipulator. The singularity of this matrix therefore means that there will be a linear dependence between these vectors. Grassmann showed that linear dependence of Plücker vectors induced

geometric relations between the associated lines, so that a set of n Plücker vectors creates a variety with dimension $m < n$. A thorough introduction to Grassmann geometry please refers to (Pottmann et al., 1999). The applications of Grassmann geometry can be found in references (Collins & Long, 1995; Hao & McCarthy, 1998; Wu et al., 2006). Using the Grassmann's geometrical conditions, an algorithm for finding the singular configurations of any type of parallel robot whose full inverse kinematic jacobian consists of Plücker vectors should be designed. Firstly consider all sets of n lines that are associated with the Plücker vectors constructed from full inverse kinematic jacobian matrices, and then the pose of the moving platform is determined so that the n lines satisfy one of the geometrical conditions which ensure that they span a variety of dimension $n-1$, thereby leading to a singularity of the robot. The following list the geometric conditions that ensure that the dimension of the variety spanned by a set of $n+1$ Plücker vectors is n , for each possible dimension n of the variety (Merlet, 2006). It should be noted that the notation of intersecting lines also include parallel lines which intersect at infinity. To consider the reading convenience, the following results is excerpted from the monograph written by Merlet (Merlet, 2006).


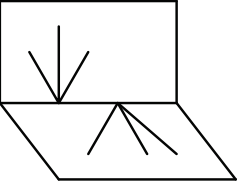
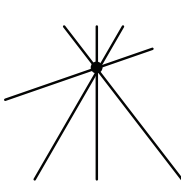
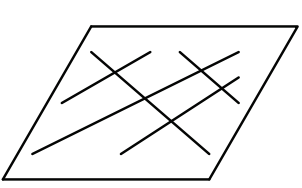
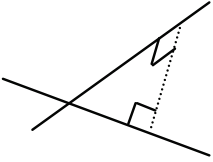

dimension	a	b	c	d
3				
2				
1				

Fig.12. Geometrical conditions that characterize the varieties of dimension 1, 2 and 3 (Merlet, 2006)

For the variety of dimension 1 (called a point) there is just one Plücker vector and one line. A variety of dimension 2, called a line, may be constituted either by two Plücker vectors for which the associated lines are skew, i.e. they do not intersect and they are not parallel, or be spanned by more than two Plücker vectors if the lines that are associated with the vectors form a planar pencil of lines, i.e. they are coplanar and possess a common point (possibly at infinity, to cover the case of coplanar parallel lines). A variety of dimension 3, called a plane, is the set of lines F that are dependent on 3 lines F_1, F_2, F_3 . It is possible to show that all the points belonging to the lines F lie on a quadric surface Q . This quadric degenerates to a pair of planes P_1, P_2 if any two of the three lines intersect.

- condition 3d: all the lines are coplanar, but do not constitute a planar pencil of lines; F_1, F_2, F_3 are coplanar and P_1, P_2 are coincident.

- condition 3c: all the lines possess a common point, but they are not coplanar; F_1, F_2, F_3 intersect at the same point, possibly at infinity (this covers the case of parallel lines).
- condition 3b: all the lines belong to the union of two planar pencils of non coplanar lines that have a line L in common; two of the lines intersect at a point \mathbf{p} , and L intersect the last line at \mathbf{a} . Two different cases may occur:
 - P_1, P_2 are distinct and intersect along the line L . The set of dependent lines are the lines in P_1 that go through \mathbf{a} , and the lines in P_2 that go through \mathbf{p}
 - P_1, P_2 are distinct and parallel. This occurs if two of the lines F_i are parallel; L is a line at infinity, and the set of dependent lines are two planes of parallel lines
- condition 3a: all the lines belong to a regulus; F_1, F_2, F_3 are skew.

A variety of dimension 4, called a congruence, corresponds to a set of lines which satisfies one of the following 4 conditions:

- condition 4d: all the lines lie in a plane or meet a common point that lies within this plane. This is a degenerate congruence.
- condition 4c: all the lines belong to the union of three planar pencils of lines, in different planes, but which have a common line. This is a parabolic congruence.
- condition 4b: all the lines intersect two given skew lines. This is a hyperbolic congruence.
- condition 4a: the variety is spanned by 4 skew lines such that none of these lines intersects the regulus that is generated by the other three. This is an elliptic congruence.

A variety of dimension 5, called a linear complex, is defined by two 3-dimensional vectors $(\mathbf{c}, \bar{\mathbf{c}})$ as the set of lines L with Plücker coordinates $(\mathbf{l}, \bar{\mathbf{l}})$ such that $\bar{\mathbf{c}} \cdot \mathbf{l} + \mathbf{c} \cdot \bar{\mathbf{l}} = 0$. The complex may be:

- condition 5b: all the lines of the complex intersect the line with Plücker coordinates $(\mathbf{c}, \bar{\mathbf{c}})$, namely, $\mathbf{c} \cdot \bar{\mathbf{c}} = 0$. This is a singular configuration.
- condition 5a: $\mathbf{c} \cdot \bar{\mathbf{c}} \neq 0$. This is a general or non singular configuration.

The degree of freedom associated with a linear complex is a screw motion with axis defined by the line with Plücker vector $(\mathbf{c}, \bar{\mathbf{c}} - p\mathbf{c})/\|\mathbf{c}\|$, where $p = \mathbf{c} \cdot \bar{\mathbf{c}}/\|\mathbf{c}\|^2$ is the pitch of the motion.

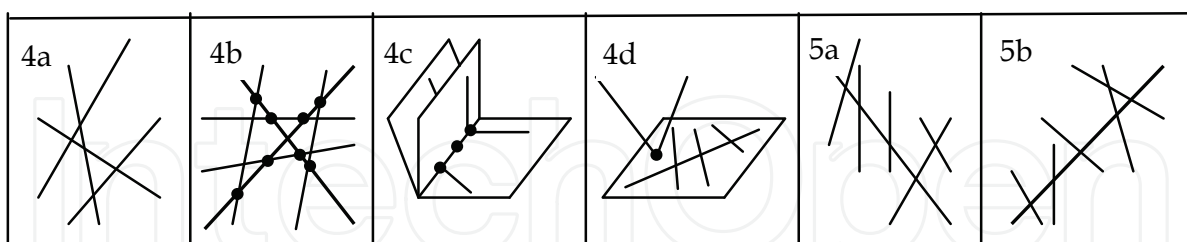


Fig.13. Geometrical conditions that characterize the varieties of dimension 4 and 5 (Merlet, 2006)

4.1.3 Screw theory

According to screw theory, the instantaneous velocities of a rigid body can be described by a 6-dimensional vector of the form $(\boldsymbol{\omega}, \mathbf{v})$, where $\boldsymbol{\omega}$ is the angular velocity of the rigid body, and \mathbf{v} is its translational velocity. These elements are called *velocity twists* or *screws*. Forces and torques exerted on the rigid body are important for motion and may be represented as a

couple of 3-dimensional vectors (\mathbf{F}, \mathbf{M}) called a *wrench*. A twist and a wrench will be said to be reciprocal if

$$\mathbf{F} \cdot \mathbf{v} + \mathbf{M} \cdot \boldsymbol{\omega} = 0 \quad (45)$$

When a kinematic chain is connected to a rigid body the key point is that the possible instantaneous twists for the rigid body are reciprocal to the wrenches imposed by the kinematic chains (called the constraint wrenches). In other words, the DOF of the rigid body are determined by the constraint wrenches. So based on linear dependency of the constraint wrenches, the singular configurations can be identified. Another function of the screw theory is the mobility analysis (Li & Huang, 2003).

4.2 Static analysis of the H4

When deriving the Jacobian matrix of the H4 using the velocity-equation formulation described in section 3.3, the result is a 4×4 Jacobian matrix because of the 4-DOF of the manipulator. However, it is not clear as to this is the best way to express the Jacobian of this type of limited-DOF parallel manipulator when singular analysis is processed. Because this approach is valid for general-purpose planar or spatial parallel manipulators, for which the connectivity of each serial chain (limb) is equal to the mobility of the end effector, it is not necessary true for parallel manipulators with less than 6-DOF (Joshi & Tsai, 2002). For example, this approach leads to a 3×3 Jacobian matrix for the 3-UPU parallel manipulator assembled for pure translation (Tsai, 1996; Tsai & Joshi, 2000). However, such a 3×3 Jacobian matrix cannot predict all possible singularities. Di Gregorio and Parenti-Castelli (Di Gregorio & Parenti-Castelli, 1999) analyzed the singularities of the 3-UPU translational platform. They derived the conditions for which the actuators cannot control the linear velocity of the moving platform, generally known as *architecture singularities*. Bonev and Zlatanov also found that under certain configurations the 3-UPU translational platform would gain rotational DOFs, which was called *constraint singularities* (Bonev and Zlatanov, 2001). Constraint singularities occur when the limbs of a limited-DOF parallel manipulator lose their ability to constrain the moving platform to the intended motion.

The 4×4 Jacobian matrix of the H4 cannot predict all possible singularities. Under certain configurations the chains of the H4 parallel manipulator lose their ability to constrain the moving platform to the intended motion, and the nacelle will gain additional DOF(s). So it is necessary to derive a full 6×6 matrix of the robot. In order to obtain the full 6×6 matrix, including the moments of constraints, one can express the set of static equilibrium conditions of the nacelle. These expressions result in a 6×8 matrix that maps the external wrench acting on the nacelle to the moments of the internal forces that are generated by the (S-S)₂ chains. Taking into account the constraint relations between the (S-S)₂ chains, we can derive a 6×6 matrix. This matrix's rows describe the six governing lines, from which the manipulator's singularities are obtained.

The structure and the geometrical parameters of the manipulator are shown in Fig.10. The static analysis of H4 manipulator can be divided into two parts. One regards the static equilibrium of the nacelle with B_1B_2 and B_3B_4 . The second deals with the static equilibrium conditions of the parallelograms which are composed of P-(S-S)₂ chains. For a P-(S-S)₂ chain, $\mathbf{A}_{i1}\mathbf{B}_{i1} = \mathbf{A}_{i2}\mathbf{B}_{i2} = \mathbf{A}_i\mathbf{B}_i$, \mathbf{A}_i and \mathbf{B}_i are centers of segments $\mathbf{A}_{i1}\mathbf{B}_{i1}$ and $\mathbf{A}_{i2}\mathbf{B}_{i2}$. Every chain has 5 DOFs, and provides the same type: 3 translations and 2 rotations. Since both rods

$A_{i1}B_{i1}$ and $A_{i2}B_{i2}$ are considered as plain solids, the impossible motion is the rotation about the vector: $\mathbf{A}_i\mathbf{B}_i \times \mathbf{u}_i$, where $\mathbf{u}_i = \mathbf{B}_{i1}\mathbf{B}_{i2}$. Observing the structure of the parallel part of the (S-S)₂ chain in Fig.2, one can detect that due to the spherical joint, there are moments exerted by the rods to B_i (the direction is along $\mathbf{A}_i\mathbf{B}_i \times \mathbf{u}_i$) and forces to B_i (the direction is along $\mathbf{B}_i\mathbf{A}_i$), the static equilibrium for the i th chain is given by (see Fig.14):

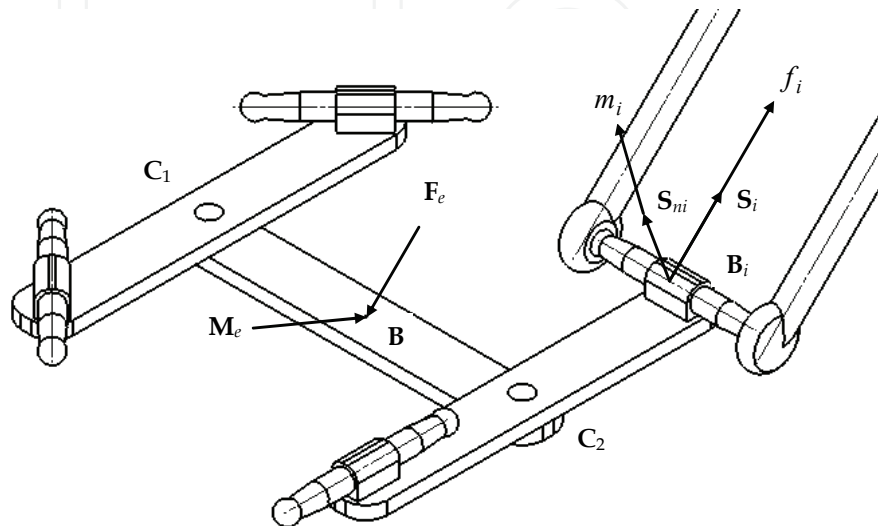


Fig.14. Forces and moments transmitted to the nacelle

$$\sum_{i=1}^4 f_i \mathbf{S}_i - \mathbf{F}_e = \mathbf{0} \quad (46)$$

$$\sum_{i=1}^4 {}^A\mathbf{R}_B \mathbf{r}_i \times \mathbf{S}_i \cdot f_i + \sum_{i=1}^4 m_i \mathbf{S}_{ni} - \mathbf{M}_e = \mathbf{0}$$

where ${}^A\mathbf{R}_B$ is a rotation matrix, which expresses the orientation of the nacelle with respect to the fixed reference frame; \mathbf{r}_i is a vector connecting B to B_i ; \mathbf{S}_i and f_i are the unit direction vectors and the internal forces acting on B_i in the direction of $\mathbf{B}_i\mathbf{A}_i$ respectively; \mathbf{S}_{ni} and m_i are the unit direction vectors and the internal moments acting on the B_i in the direction of $\mathbf{A}_i\mathbf{B}_i \times \mathbf{u}_i$. Writing equation (46) in a matrix form yields:

$$\begin{bmatrix} \mathbf{S}_1 & \mathbf{S}_2 & \mathbf{S}_3 & \mathbf{S}_4 & \mathbf{0} & \mathbf{0} & \mathbf{0} & \mathbf{0} \\ {}^A\mathbf{R}_B \mathbf{r}_1 \times \mathbf{S}_1 & {}^A\mathbf{R}_B \mathbf{r}_2 \times \mathbf{S}_2 & {}^A\mathbf{R}_B \mathbf{r}_3 \times \mathbf{S}_3 & {}^A\mathbf{R}_B \mathbf{r}_4 \times \mathbf{S}_4 & \mathbf{S}_{n1} & \mathbf{S}_{n2} & \mathbf{S}_{n3} & \mathbf{S}_{n4} \end{bmatrix} \begin{bmatrix} f_1 \\ f_2 \\ f_3 \\ f_4 \\ m_1 \\ m_2 \\ m_3 \\ m_4 \end{bmatrix} = \begin{bmatrix} \mathbf{F}_e \\ \mathbf{M}_e \end{bmatrix} \quad (47)$$

the matrix in the left of equation (47) is a 6×8 matrix. In order to obtain the 6×6 matrix, the constraint relations between $f_i, m_i (i = 1, 2, 3, 4)$ should be analyzed.

Link C_1C_2 is connected, on one side, to B_1B_2 by a revolute joint whose direction is represented by vector \mathbf{v}_1 , on the other side, to B_3B_4 by a revolute joint whose direction is represented by vector \mathbf{v}_2 . Thus, we can consider two 5-DOF “meta-chains” on each side of the nacelle. Those “meta-chains” have the following properties (Pierrot & Company, 1999):

- First “meta-chain”: the rotation about $(\mathbf{S}_{n1} \times \mathbf{S}_{n2}) \times \mathbf{v}_1$ is impossible.
- Second “meta-chain”: the rotation about $(\mathbf{S}_{n3} \times \mathbf{S}_{n4}) \times \mathbf{v}_2$ is impossible.

So, the moment's direction exerted by B_1B_2 to C_1C_2 is along $(\mathbf{S}_{n1} \times \mathbf{S}_{n2}) \times \mathbf{v}_1$, and the moment's direction exerted by B_3B_4 to C_1C_2 is along $(\mathbf{S}_{n3} \times \mathbf{S}_{n4}) \times \mathbf{v}_2$. The static equilibrium of C_1C_2 is given by (see Fig.15):

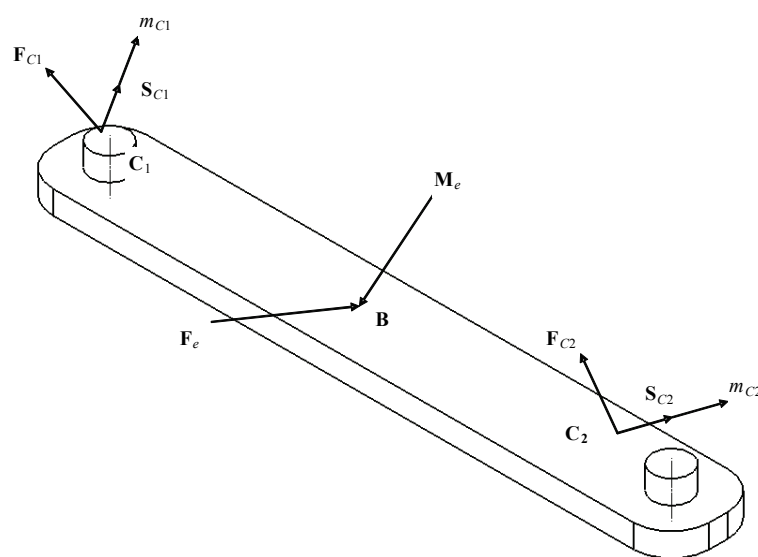


Fig.15. Forces and moments transmitted to C_1C_2

$$\begin{aligned} \mathbf{F}_{C1} + \mathbf{F}_{C2} &= \mathbf{F}_e \\ \mathbf{BC}_1 \times \mathbf{F}_{C1} + \mathbf{BC}_2 \times \mathbf{F}_{C2} + m_{C1} \mathbf{S}_{C1} + m_{C2} \mathbf{S}_{C2} &= \mathbf{M}_e \end{aligned} \quad (48)$$

where

$$\begin{aligned} \mathbf{F}_{C1} &= f_1 \mathbf{S}_1 + f_2 \mathbf{S}_2 \\ \mathbf{F}_{C2} &= f_3 \mathbf{S}_3 + f_4 \mathbf{S}_4 \end{aligned} \quad (49)$$

are the internal force vectors acting on the points C_1 and C_2 , m_{C1} and m_{C2} are moments transmitted to C_1C_2 ; \mathbf{S}_{C1} and \mathbf{S}_{C2} are the unit vectors along the direction of $(\mathbf{S}_{n1} \times \mathbf{S}_{n2}) \times \mathbf{v}_1$ and $(\mathbf{S}_{n3} \times \mathbf{S}_{n4}) \times \mathbf{v}_2$ respectively.

Introducing expressions (49) into equation (48) becomes as follows:

$$\begin{aligned} \sum_{i=1}^4 f_i \mathbf{S}_i - \mathbf{F}_e &= 0 \\ {}^A \mathbf{R}_B \mathbf{BC}_1 \times \left(\sum_{i=1}^2 \mathbf{S}_i f_i \right) + {}^A \mathbf{R}_B \mathbf{BC}_2 \times \left(\sum_{i=3}^4 \mathbf{S}_i f_i \right) + \sum_{i=1}^2 m_{Ci} \mathbf{S}_{Ci} - \mathbf{M}_e &= 0 \end{aligned} \quad (50)$$

Writing equation (50) in a matrix form yields:

$$\begin{bmatrix} \mathbf{S}_1 & \mathbf{S}_2 & \mathbf{S}_3 & \mathbf{S}_4 & \mathbf{0} & \mathbf{0} \\ {}^A\mathbf{R}_B\mathbf{l}_1 \times \mathbf{S}_1 & {}^A\mathbf{R}_B\mathbf{l}_1 \times \mathbf{S}_2 & {}^A\mathbf{R}_B\mathbf{l}_2 \times \mathbf{S}_3 & {}^A\mathbf{R}_B\mathbf{l}_2 \times \mathbf{S}_4 & \mathbf{S}_{C1} & \mathbf{S}_{C2} \end{bmatrix} \begin{bmatrix} f_1 \\ f_2 \\ f_3 \\ f_4 \\ m_{C1} \\ m_{C2} \end{bmatrix} = \begin{bmatrix} \mathbf{F}_e \\ \mathbf{M}_e \end{bmatrix} \quad (51)$$

where $\mathbf{l}_1 = \mathbf{BC}_1, \mathbf{l}_2 = \mathbf{BC}_2$. The forces and moments at the robot joints due to external load are given by:

$$\mathbf{J}_S^{-1} \begin{bmatrix} \mathbf{F}_e \\ \mathbf{M}_e \end{bmatrix} = \begin{bmatrix} f_1 \\ f_2 \\ f_3 \\ f_4 \\ m_{C1} \\ m_{C2} \end{bmatrix} \quad (52)$$

Investigating the transformation matrix \mathbf{J}_S given in equation (52), one can analyze the singularity of the parallel part. The columns of \mathbf{J}_S are lines lying on the *Klein quadric* M_2^4 , as they satisfy Klein's equation (Hunt, 1978):

$$l_1l_4 + l_2l_5 + l_3l_6 = 0 \quad (53)$$

where each column of equation (53) is represented by its Plücker line coordinates given by $(l_1, l_2, l_3, l_4, l_5, l_6)^T$.

Moreover, considering the forces and moments exerted on the actuator, one can obtain (see Fig.16).

$$\tau_i \mathbf{k}_z + \sigma_i \mathbf{k}_{pi} = f_i \mathbf{S}_i \quad (54.1)$$

$$f_i \cos \theta_i = \tau_i \quad (54.2)$$

$$f_i \sin \theta_i = \sigma_i \quad (54.3)$$

$$\cos \theta_i = \mathbf{k}_z \cdot \mathbf{S}_i \quad (54.4)$$

where \mathbf{k}_{pi} is the unit vector along the direction $(\mathbf{k}_z \times \mathbf{u}_i)$. Equation (54.2) can be written for $i=1,2,3,4$, and the results grouped in a matrix form, τ_i can be written as:

$$\mathbf{J}_P \begin{bmatrix} f_1 \\ f_2 \\ f_3 \\ f_4 \end{bmatrix} = \begin{bmatrix} \tau_1 \\ \tau_2 \\ \tau_3 \\ \tau_4 \end{bmatrix} \quad (55)$$

where

$$\mathbf{J}_P = \begin{bmatrix} \cos \theta_1 & 0 & 0 & 0 \\ 0 & \cos \theta_2 & 0 & 0 \\ 0 & 0 & \cos \theta_3 & 0 \\ 0 & 0 & 0 & \cos \theta_4 \end{bmatrix} \tag{56}$$

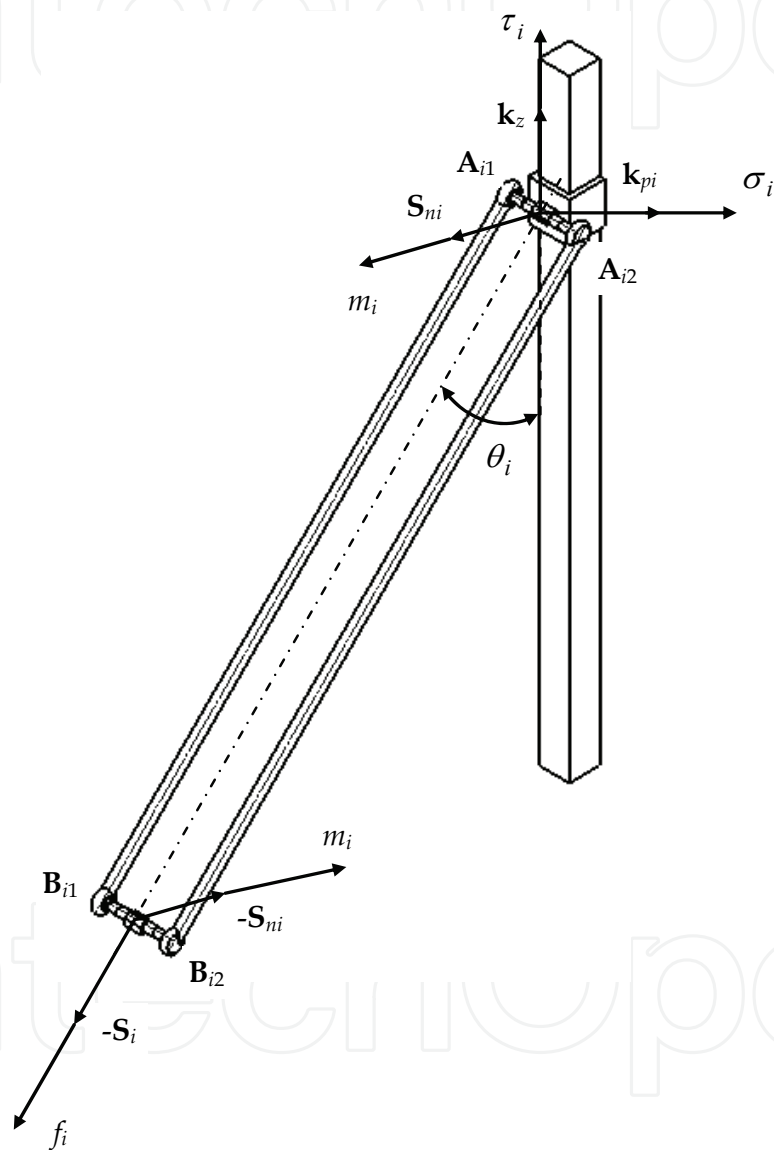


Fig.16. Parallelogram static analysis

\mathbf{J}_S (equation (52)) and \mathbf{J}_P (equation (56)) provide the information about the singularities of the H4 manipulator. The analysis of \mathbf{J}_S provides the singularity of the parallel part of H4 robot known as the “parallel singularity” and \mathbf{J}_P provides the singularity due to the parallelogram structure, known as the “serial singularity”. In (Liu et al., 2003), the singularity caused by \mathbf{J}_P is also called as “actuator singularity”.

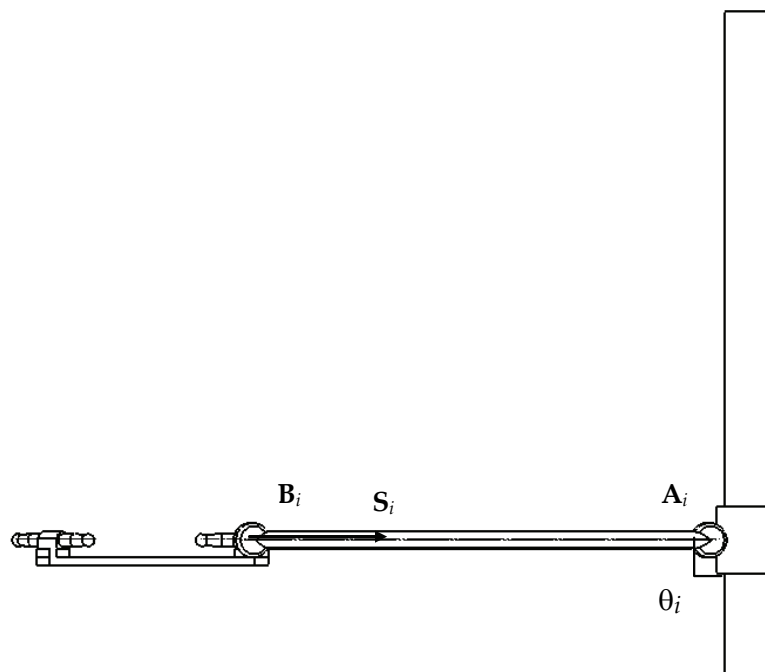


Fig.17. Serial singularity of H4 manipulator

Observing \mathbf{J}_p one can see that singularity occurs whenever $\theta_i = \pi/2 + \pi k$ ($k=1, \dots, n$, $i=1,2,3,4$). In this case one or more columns of \mathbf{J}_p are zero and the nacelle can't move in the S_i direction, namely, the manipulator loses a DOF. Fig.17 shows the serial singularity of H4 manipulator.

4.3 The behavior of the H4 manipulator in parallel singular configurations

The parallel singular configurations of the H4 are identified by investigating matrix \mathbf{J}_s . The first four columns of \mathbf{J}_s define the four internal forces of parallelogram which are along the direction $\mathbf{B}_i\mathbf{A}_i$ (see Fig.53 and 55). Utilizing Grassmann geometry, we can obtain all singularities of \mathbf{J}_s .

Based on H4's kinematic architecture, the first four columns of \mathbf{J}_s can form only the following linear varieties:

- Type I: a line bundle where all lines intersect a common point, but they are not coplanar. This is the condition 3c described in section 4.1.2.
- Type II: all the lines belong to the union of two planar pencils of non coplanar lines that have a line in common. This is the condition 3b described in section 4.1.2.

Type I can be considered as the special condition of Type II. When the first four columns of \mathbf{J}_s are linear dependent, the actuators can't control the linear velocity of the nacelle, generally known as "*architecture singularity*" (Joshi & Tsai, 2002).

The last two columns of \mathbf{J}_s define the two moments of constraint which are along the direction \mathbf{S}_{Ci} . We make here the assumption that the two revolute joints placed on the nacelle have the same direction represented by vector \mathbf{v} . This choice may be not the only one, but it worth noting that placing two revolute joints parallel to each other on the nacelle

is a good choice for practical matters. The existence of a rotational motion about \mathbf{v} can be written as follows (Pierrot & Company, 1999):

$$\mathbf{S}_{C1} \times \mathbf{S}_{C2} \neq \mathbf{0} \quad (57)$$

When $\mathbf{S}_{C1} \times \mathbf{S}_{C2} = \mathbf{0}$, the vectors \mathbf{S}_{C1} and \mathbf{S}_{C2} are linearly dependent. The constraint moments exerted on the nacelle are along the same direction, and the robot would gain additional DOF(s). This singularity arises from deficiency of constraints, so we call this singularity as “*constraint singularity*”.

In order to investigate the instantaneous motion the robot tends to perform while in singular configurations, the LCAA which was presented at (Pottmann et al., 1999) and further used for robotic analysis in (Wolf & Shoham, 2003) is adopted. The LCAA is based on determining the linear complex $\mathbf{C} = (\mathbf{c}, \bar{\mathbf{c}})$, which is the closest one to the given set of lines $\mathbf{L}_i = (\mathbf{l}_i, \bar{\mathbf{l}}_i)$. The moment of \mathbf{L}_i with respect to a linear complex \mathbf{C} is given by:

$$m(\mathbf{L}, \mathbf{C}) = \frac{|\bar{\mathbf{c}} \cdot \mathbf{l}_i + \mathbf{c} \cdot \bar{\mathbf{l}}_i|}{\|\mathbf{c}\|} \quad (58)$$

Hence, given a set of lines \mathbf{L}_i , the closest linear complex among all linear complexes χ can be given by the minimization of:

$$\sum_{i=1}^k m(\mathbf{L}_i, \chi) \quad (59)$$

where χ is given by $\chi = (\mathbf{x}, \bar{\mathbf{x}}) \in \mathfrak{R}^6$.

Equation (59) is equivalent to minimizing the positive semi-definite quadratic form given by (Pottmann et al., 1999):

$$F(\mathbf{X}) = \sum_{i=1}^k (\bar{\mathbf{x}} \cdot \mathbf{l}_i + \mathbf{x} \cdot \bar{\mathbf{l}}_i)^2 = \chi^T \mathbf{M} \chi \quad (60)$$

under the normalization condition $1 = \|\mathbf{x}\|^2 = \chi^T \mathbf{D} \chi$, where $\mathbf{D} = \text{diag}(1, 1, 1, 0, 0, 0)$, χ presents the set of all linear complexes given by $\chi = (\mathbf{x}, \bar{\mathbf{x}}) \in \mathfrak{R}^6$, and \mathbf{M} is the Gramian matrix of \mathbf{J}_s . Equation (60) is a general eigenvalue problem and the solution, \mathbf{C} , is the eigenvector χ_i corresponding to the smallest eigenvalue. Moreover, given the closest linear complex found by the algorithm, the axis, \mathbf{A} , of the linear complex and its pitch can also be revealed. In fact, the minimization procedure shown in above minimizes the work of the wrench applied on the moving platform and the twists. When the smallest eigenvalue is zero, there is no work generated by the set of wrenches when the platform moves in the twist direction given by χ . So we can use LCAA to investigate the behavior of H4 manipulator in singular configurations.

4.4 Simulation and results

In this section, the parallel singularities of an example H4 manipulator are presented and the LCAA method is used to investigate the instantaneous motion the manipulator tends to

perform while in these singular configurations. For simulation, the design parameters we have selected is described in Fig.11, where the parameters have been chosen as described in section 3.2.2.

Architecture singularities

Architecture singular configurations of the H4 manipulator are identified using line geometry (Merlet, 2006). Note the first four columns of \mathbf{J}_S as:

$$\begin{bmatrix} \mathbf{S}_1 & \mathbf{S}_2 & \mathbf{S}_3 & \mathbf{S}_4 \\ {}^B\mathbf{R}_D\mathbf{I}_1 \times \mathbf{S}_1 & {}^B\mathbf{R}_D\mathbf{I}_1 \times \mathbf{S}_2 & {}^B\mathbf{R}_D\mathbf{I}_2 \times \mathbf{S}_3 & {}^B\mathbf{R}_D\mathbf{I}_2 \times \mathbf{S}_4 \end{bmatrix} = \begin{bmatrix} a_1 & a_2 & a_3 & a_4 \\ \bar{a}_1 & \bar{a}_2 & \bar{a}_3 & \bar{a}_4 \end{bmatrix} = [\mathbf{A}_1 \ \mathbf{A}_2 \ \mathbf{A}_3 \ \mathbf{A}_4] \tag{61}$$

where $\|a_i\|=1$ and $a_i \cdot \bar{a}_i = 0$, so the six coordinates with (a_i, \bar{a}_i) are called the normalized Plücker coordinates of \mathbf{A}_i ($i=1,2,3,4$). Deriving from the geometric conditions (Type I and Type II) in section 4.3, we can find that when the coordinates of point D satisfy the following condition:

$$\begin{aligned} x &= -9.5812 \\ y &= -9.4130 \\ \theta &= -1.5080 \end{aligned} \tag{62}$$

singularity occurs. The closest linear complex's axis found by the algorithm is:

$$\mathbf{A} = [0 \quad 0 \quad 1 \quad -5.2937 \quad -0.3331 \quad 0]$$

The standard deviation of the lines form \mathbf{C} is given by: $\sigma = \sqrt{\frac{\lambda_i}{k-5}} = 0$, and the linear complex's pitch is given by: $p = \frac{\mathbf{c} \cdot \bar{\mathbf{c}}}{\mathbf{c}^2} = -9.4047$. Fig.18 demonstrated the result of the LCAA.

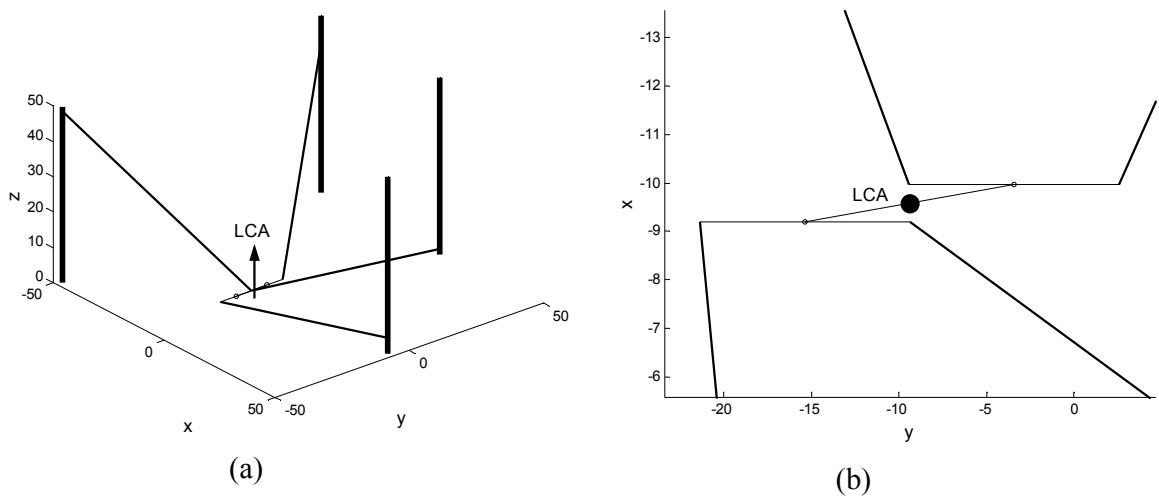


Fig.18. H4 robot with linear complexes (a): 3D view (b): top view

Corresponding to the non-zero pitch value of the linear complex, at this singularity the robot performs a screw motion of rotation and translation around the linear complex axis \mathbf{A} .

Constraint singularities

From the discussion in section 4.3, we know that when $\mathbf{S}_{C1} \times \mathbf{S}_{C2} = \mathbf{0}$, the robot is in a constraint singular configuration. If we select the structure parameters as Fig.11, when:

$$\begin{aligned} x &= -3.6683 \\ y &= 3.3709 \\ \theta &= -2.3905 \end{aligned} \quad (63)$$

the robot reaches singular configuration.

Constraint singularity occurs in limited-DOF manipulator when the screw system, formed by the constraint wrenches in all chains, loses rank. In this section, the geometric explanation of constraint singularity is given, then LCAA is applied to investigate the behavior of H4 manipulator in constraint singular configuration. From the viewpoint in (Zlatanov et al., 2002), the system of the constraining wrenches of H4, \mathcal{W} , contains as a subspace the 2-system of all pure moments. Then its reciprocal system, the freedoms system \mathcal{T} , must contain 3 translations and 1 rotation. In a H4 manipulator, the two “meta-chain” constrain system \mathcal{W}_p contains two pure moments, one’s direction is along \mathbf{S}_{C1} , and the other’s direction is along \mathbf{S}_{C2} . When the two moments of the two “meta-chain” are linearly independent, two pure moments will be in \mathcal{W} .

However, in the constraint singular configuration, \mathbf{S}_{C1} and \mathbf{S}_{C2} are parallel. The constraining moments of two “meta-chain” are identical and the system \mathcal{W}_p are the same one-system. Then, \mathcal{W} consists of only one screw. Hence, the twist system of the robot is a five-system and the mechanism gains new additional freedom. Applying the method of the closest linear complex on the H4 robot in its constraint singular configuration, we can find the closest linear complex’s axis is: $\mathbf{A} = [0.9137 \quad 0.3524 \quad -0.2024 \quad 0.3208 \quad -0.2064 \quad 1.0887]$

and the linear complex’s pitch is: $p = \frac{\mathbf{c} \cdot \bar{\mathbf{c}}}{\mathbf{c}^2} = 1.0469$. $\mathbf{S}_{C1} = -\mathbf{S}_{C2} = [0.3599 \quad -0.9330 \quad 0]^T$ means

that this configuration is singular and the robot is able to execute a screw motion of rotation and translation around the linear complex axis. The direction of the linear complex axis is perpendicular to \mathbf{S}_{C1} (and \mathbf{S}_{C2}) because $\mathbf{a} \cdot \mathbf{S}_{C1} = 0$ (and $\mathbf{a} \cdot \mathbf{S}_{C2} = 0$). This corroborates the results deduced from the viewpoint of constraint singularities. Fig.19 demonstrates the result of the LCAA in constraint singular configurations.

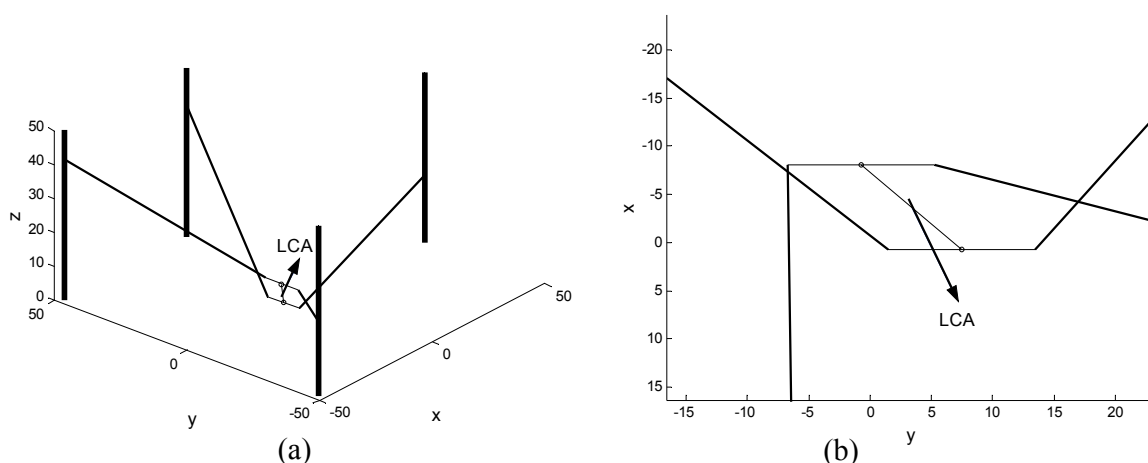


Fig.19. H4 robot with linear complexes (a): 3D view (b): top view

Discussion: Simulation Results of the H4 robot

From above discussion, only one architecture singular configuration can be found. In this configuration, the intersection point of $\mathbf{A}_1, \mathbf{A}_2$ and the intersection point of $\mathbf{A}_3, \mathbf{A}_4$ (see equation (61)) are superposed, which satisfies the geometric condition of Type I (in section 4.3). However, for constraint singularities, as long as $\mathbf{S}_{C1} \times \mathbf{S}_{C2} = \mathbf{0}$ is satisfied, the manipulator would reach singular configurations. Four parameters x, y, z, θ are used to describe the configuration of a H4 manipulator. z is independent of the singularities. The singular equation $\mathbf{S}_{C1} \times \mathbf{S}_{C2} = \mathbf{0}$ provides only one constraint equation, so the three parameters x, y, θ constitute a three dimension curved surface. All the points in the curved surface satisfy the equation $\mathbf{S}_{C1} \times \mathbf{S}_{C2} = \mathbf{0}$. We call this surface as constraint singular surface. The equation of the constraint singular surface can be written as:

$$(\mathbf{S}_{C1} \times \mathbf{S}_{C2}) \cdot \mathbf{v} = 0 \quad (64)$$

Fig.20 depicts the constraint singular surface.

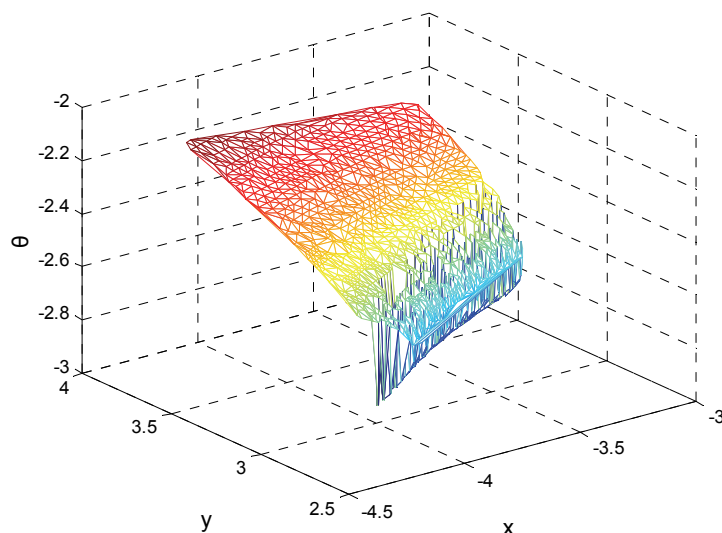


Fig.20. The constraint singular surface

As we can see from the reference (Wolf & Shoham, 2003):

$$F(\mathbf{X}) = \sum_{i=1}^k (\bar{\mathbf{x}} \cdot \mathbf{l}_i + \mathbf{x} \cdot \bar{\mathbf{l}}_i)^2 = \boldsymbol{\chi}^T \mathbf{M} \boldsymbol{\chi} = \lambda$$

λ has the meaning of the sum of the square of the virtual work generated by the structure to the nacelle, when the latter is moving instantaneously in the twist direction given by $\boldsymbol{\chi}$. Hence, if $\lambda = 0$, the chains would lose the constraints on the nacelle and the nacelle could move instantaneously in the twist direction given by $\boldsymbol{\chi}$.

The standard deviation of the lines \mathbf{L}_i from \mathbf{C} , may be written as:

$$\sigma = \sqrt{\frac{\lambda}{k-5}} = \sqrt{\frac{\sum_{i=1}^k m(\mathbf{L}_i, \mathbf{c})^2}{k-5}}$$

which is the square of error from L_i to C . In case of a sufficiently small deviation σ , the given lines L_i can be well approximated by lines of the linear complex C , which means that the current configuration is close to the singular configuration. When $\sigma = 0$, the lines L_i lie on the linear complex C , which means that the manipulator is in a singular configuration and the nacelle can move in the twist direction of the linear complex axis. In order to investigate the robot's behavior in the vicinity of the singular configuration, a simulation is performed in the neighborhood of the architecture singular configuration (Fig.21-Fig.22).

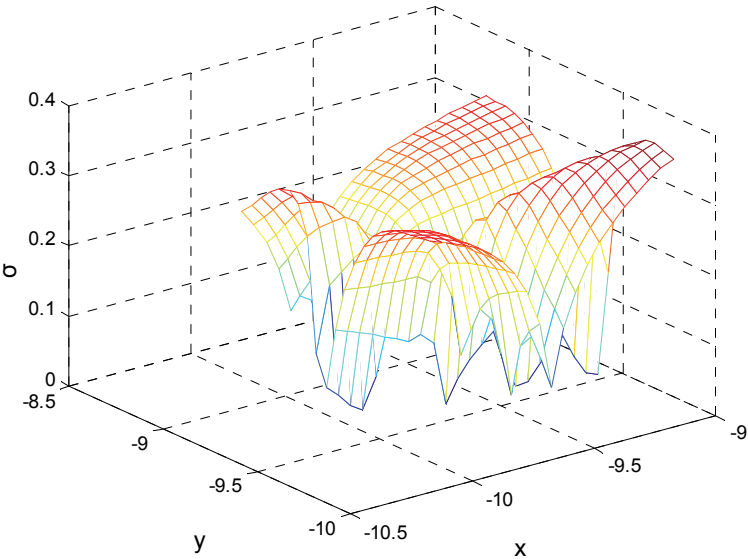


Fig.21. Minimum σ in the vicinity of the architecture singular configuration

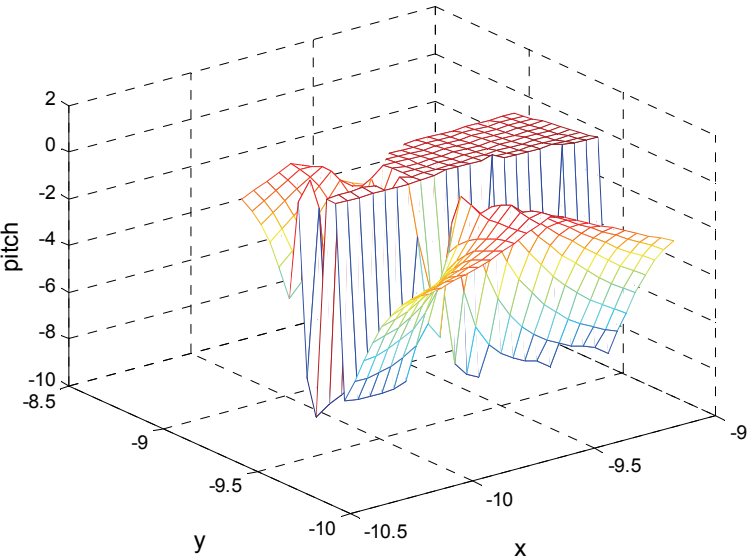


Fig.22 Pitch of linear complex with minimum σ in the vicinity of the architecture singular configuration

All the simulations are in the adjacent range of the singular configuration: $x \in [-10.1 \quad -9.1]$, $y \in [-9.9 \quad -8.9]$, $z = 0$, $\theta = -1.5080$.

It can be seen that the manipulator is no longer in a singular position. However, when manufacturing tolerances are greater than the value σ , there is still possibility of an uncontrolled motion of the nacelle according to the interpretation of σ .

5. Conclusions

This chapter mainly discusses the architectures and some kinematic problems about the 4-DOF parallel manipulator H4 which is suitable for pick and place operations. The geometric methods used to analyze the singularity poses are introduced in detail. As this type of parallel manipulator generally performs tasks implying significant accuracy, velocities and accelerations, there are still numerous topics need further study.

It is the complexity of the parallel manipulator's implantation, of their control and of their design that hinders their widely use. Control efficiency is related to kinematics calculation. Although the analytical formulation of the direct kinematics is deduced in section 3.2.1, solving the 16th degree univariate polynomial equation is not trivial and efficient control still requires very fast algorithms which give all of the solutions.

The motions of H4 are mainly restricted by mechanical limits on passive joints, interference links and limitations due to the actuators. Because of the coupling between translations and rotations, it is generally complex to determine the workspace of H4. There are various methods can be used to calculate the workspace of H4, such as the discretization approach, inequality constraints approach (Jo, 1989) and algebraic approach (Husty, 1996). Merlet (Merlet, 2006) has pointed out that the geometrical approaches are very efficient for the determination of various types of workspace and algebraic geometry should also play an important role in some of the algorithms which are used to calculate the workspace of parallel manipulators.

Singularity analysis of parallel manipulators is crucial for practical applications. Besides the geometric method suggested in section 4, some new ideas are provided to analyze singularities of parallel manipulators by using different mathematic tools. Differential geometric is a powerful tool for general analysis of parallel manipulators. From the geometric properties of the parallel manipulator, Liu et al. presented a framework for analyzing the singularities of a parallel manipulator (Liu et al., 2003). Topological structure of these singularities and their relations with the kinematic parameters of the system were investigated systematically using Morse function theory. An intrinsic definition of parameterization singularities was given in this chapter. Due to the profound explanation of the parallel manipulators' characteristics, although the differential geometric tool is abstract, its use for general analysis and extension to geometric control of parallel manipulator is still worthy of study. In some situations, it is only necessary to seek singular configurations in the workspace of parallel manipulators. Su et al. (Su et al., 2003) proposed a new singularity analysis method for Steward platform using genetic algorithm (GA). The square of determinant of the Jacobian matrix is selected as the objective function, and the minimal of this objective function is searched in the workspace of Steward platform by the GA. The singularity of Steward platform depends on this minimal objective function: if this value is

zero, the singularity of Steward platform will take place, otherwise, the Steward platform is singularity-free. This method can be used to determine the dimensioning of a H4 so that it is singularity-free, at least in a given workspace. Of course, the effectiveness and speediness of the GA are the chief problems which should be considered.

The study of the novel parallel manipulator H4 and its various reformative structures has become increasingly important during recent years for its excellent performance of velocity and acceleration. But numerous problems still remain open, especially the positioning accuracy of the end-effector. From the paper written by Renaud et al. (Renaud et al., 2003), the positioning accuracy of a H4 can only reach lower than 0.5mm, which cannot meet the requirements (generally lower than 0.05mm) of the semiconductor end-package equipments. We hope that this chapter will arise some attention to extend this type of parallel manipulators to semiconductor industry.

6. Acknowledgements

The work is supported by the Natural Science Fund of China (NSFC) (Project No. 50625516) and the National Fundamental Research Program (973) (Project No. 2003CB716207 and 2007CB714000).

7. References

- Agrawal, S.K.; Desmier, G. & Li, S. (1995). Fabrication and analysis of a novel 3 DOF parallel wrist mechanism. *ASME Journal of Mechanical Design*, Vol. 117, June, pp. 343-345
- Angeles, J.; Morozov, A. & Navarro, O. (2000). A novel manipulator architecture for the production of scara motions, *Proceedings of IEEE International Conference on Robotics and Automation*, pp. 2370-2375, San Francisco, USA, April 2000
- Angeles, J. (2005). The degree of freedom of parallel robots: a group-theoretic approach, *Proceedings of IEEE International Conference on Robotics and Automation*, pp. 1017-1024, Barcelona, Spain, April 2005
- Basu, D. & Ghosal, A. (1997). Singularity analysis of platform-type multi-loop spatial mechanisms. *Mechanism and Machine Theory*, Vol. 32, No. 3, pp. 375-389
- Benov, I. (2001). Delta parallel robot - the story of success. May, 6, <http://www.parallemic.org/Reviews/Review002.html>
- Bonev, L. & Zlatanov, D. (2001). The mystery of the singular SUN translational parallel robot. June, 12, 2001, <http://www.parallemic.org/Reviews/Review004.html>
- Bonev, I.A. et al. (2001). A closed-form solution to the direct kinematics of nearly general parallel manipulators with optimally located three linear extra sensors. *IEEE Transaction on Robotics and Automation*, Vol. 17, No. 2, pp. 148-156
- Bottema, O. & Roth, B. (1990). Theoretical kinematics. New York: Dover Publications
- Brogardh, T. PKM research - important issues, as seen from a product development perspective at ABB robotics, *Workshop on Fundamental Issues and Future Research Directions for parallel Mechanisms and Manipulators*, Quebec, Canada, 2002

- Bruyninckx, H. (1997). The 321-hexa: a fully parallel manipulator with closed-form position and velocity kinematics, *Proceedings of IEEE Conference on Robotics and Automation*, pp. 2657-2662, Albuquerque, April, 1997
- Carretero, J.A.; Podhorodeski, R.P.; Nahon, M.A. & Gosselin, C.M. (2000). Kinematic analysis and optimization of a new three degree-of-freedom spatial parallel manipulator. *ASME Journal of Mechanical Design*, Vol. 122, pp. 17-24
- Chablat D, D.; Wenger, P. Design of a three-axis isotropic parallel manipulator for machining applications: the orthoglide, *Workshop on Fundamental Issues and Future Research Directions for Parallel Mechanisms and Manipulators*, Quebec, Canada, Oct., 2002
- Cheung, J.W.F.; Hung, Y.S. & Widdowson, G.P. (2002). Design and analysis of a novel 4-dof parallel manipulator for semiconductor applications, *Proceedings of the 8th Mechatronics Forum International Conference*, pp. 1358-1366, Twente, Netherlands: Drebbe Institute for Mechatronics
- Chiu, Y.J. & Perng, M-H. (2001). Forward kinematics of a general fully parallel manipulator with auxiliary sensors. *International Journal of Robotics Research*, Vol. 20, No. 5, pp. 401-414
- Choi, H.-B.; Konno, A. & Uchiyama, M. (2003). Closed-form solutions for the forward kinematics of a 4-DOFs parallel robot H4, *Proceedings of IEEE/RSJ International Conference on Intelligent Robots and Systems*, pp. 3312-3317, Las Vegas, USA, October, 2003
- Clavel, R. (1988). DELTA, a fast robot with parallel geometry, *Proceedings of the 18th International Symposium on Industrial Robot*, pp. 91-100, April, 1988, Lausanne
- Collins, C.L. & Long, G.L. (1995). The singularity analysis of an in-parallel hand controller for force-reflected teleoperation. *IEEE Transactions on Robotics and Automation*, Vol. 11, No. 5, pp. 661-669
- Company, O. & Pierrot, F. (1999). A new 3T-1R parallel robot, *Proceedings of the 9th International Conference on Advanced Robotics*, pp. 557-562, October, 1999, Tokyo, Japan
- Company, O.; Marquet, F. & Pierrot F. (2003). A new high-speed 4-DOF parallel robot synthesis and modeling issues. *IEEE Transactions on Robotics and Automation*, Vol. 19, No. 3, pp. 411-420
- Company, O.; Pierrot, F. & Fouroux, J.C. (2005). A method for modeling analytical stiffness of a lower mobility parallel manipulator, *Proceedings of IEEE International Conference on Robotics and Automation*, pp. 18-22, Barcelona, Spain, April, 2005, Milan, September, 1995
- Di Gregorio, R. & Parenti-Castelli, V. (1999). Mobility analysis of the 3-UPU parallel mechanism assembled for a pure translational motion, *Proceedings of the IEEE/ASME International Conference on Advanced Intelligent Mechatronics*, pp. 520-525, Atlanta, GA, September, 1999
- Fattah, A. & Kasaei, G. (2000). Kinematics and dynamics of a parallel manipulator with a new architecture. *Robotica*, Vol. 18, pp. 535-543

- Faugère, J.C. & Lazard, D. (1995). The combinatorial classes of parallel manipulators. *Mechanism and Machine Theory*, Vol. 30, No. 6, pp. 765-776
- Feng-Cheng, Y. & Haug, E.J. (1994). Numerical analysis of the kinematic working capability of mechanism. *ASME Journal of Mechanical Design*, Vol. 116, pp. 111-117
- Funabashi, H. & Takeda, Y. (1995). Determination of singular points and their vicinity in parallel manipulators based on the transmission index, *Proceedings of the Ninth World Congress on the Theory of Machine and Mechanism*, pp. 1977-1981,
- Gosselin, C.M. & Angeles, J. (1989). The optimum kinematic design of a spherical three-degree-of-freedom parallel manipulator. *ASME Journal of Mechanisms, Transmission and Automation in Design*, Vol.111, No.2, pp. 202-207
- Gosselin, C. & Angeles, J. (1990). Singularity analysis of closed-loop kinematic chains. *IEEE Transaction on Robotics and Automation*, Vol. 6, No. 3, pp. 281-290
- Gosselin, C. (1990). Dexterity indices for planar and spatial robotic manipulators. *Proceedings of the IEEE International Conference on Robotics and Automation*, pp. 650-655, Cincinnati, May, 1990
- Gosselin, C. (1996). Parallel computational algorithms for the kinematics and dynamics of planar and spatial parallel manipulators. *ASME Journal of Dynamic Systems, Measurement and Control*, Vol. 118, No. 1, pp. 22-28
- Gosselin, C.M. & St-Pierre, É. (1997). Development and experimentation of a fast 3-DOF camera-orienting device. *The International Journal of Robotics Research*, Vol.16, No.5, pp. 619-629
- Gough, V.E. (1956). Contribution to discussion of papers on research in automobile stability, control and tyre performance, *Proceedings of the Automotive Division of the Institution of Mechanical Engineers*, Part D, pp. 392-394
- Gregorio, R. D. (2001). A new parallel wrist using only revolute pairs: the 3-RUU wrist. *Robotica*, Vol. 19, pp. 305-309
- Hao, F. McCarthy, J.M. (1998). Conditions for line-based singularities in spatial platform manipulators. *Journal of Robotic Systems*, Vol. 15, No. 1, pp. 43-55
- Hesselbach, J. & Kerle, H. (1995). Structurally adapted kinematic algorithms for parallel robots up to six degrees of freedom (dof), *Proceedings of the 9th World Congress on the Theory of Machines and Mechanisms*, pp. 1935-1939, Milan, Italy, August, 1995
- Hunt, K.H. (1978). Kinematic geometry of mechanism. Department of Mechanical Engineering, Monash University, Clayton, Victoria, Australia
- Husty, M.L. (1996). On the workspace of planar three-legged platforms. *Proceedings of the World Automation Congress*, Vol. 3, pp. 339-344, Montpellier, May, 1996
- Jo, D.Y. & Haug, E.J. (1989). Workspace analysis of closed loop mechanism with unilateral constraints. *Proceedings of the ASME Design Automation Conference*, pp. 53-60, Montreal, September, 1989
- Joshi, S.A. & Tsai L.-W. (2002) Jacobian analysis of limited-dof parallel manipulators. *ASME Journal of Mechanical Design*, Vol. 124, No. 2, pp. 254-258

- Kim, D.; Chung, W. & Youm, Y. (2000). Analytic jacobian of in-parallel manipulators. *Proceedings of IEEE International Conference on Robotics and Automation*, pp. 2376-2381, San Francisco, April, 2000
- Kim, S.-G. & Ryu, J. (2003). New dimensionally homogeneous jacobian matrix formulation by three end-effector points for optimal design of parallel manipulators. *IEEE Transactions on Robotics and Automation*, Vol. 19, No. 4, pp. 731-736
- Krut, S.; Company, O. & Benoit, M. et al. (2003). I4: a new parallel mechanism for scara motions, *Proceedings of IEEE International Conference on Robotics and Automation*, pp. 1875-1880, Taipei, Taiwan, September, 2003
- Krut, S.; Nabat, V.; Company, O. & Pierrot, F. (2004). A high-speed parallel robot for scara motions, *Proceedings of IEEE International Conference on Robotics and Automation*, pp. 4109-4115, New Orleans, USA, April, 2004
- Li, Q. & Huang, Z. (2003). Mobility analysis of lower-mobility parallel manipulators based on screw theory, *Proceeding of IEEE International Conference on Robotics and Automation*, pp. 1179-1184, Taipei, Taiwan, September, 2003
- Liu, G.F.; Lou, Y.J. & Li, Z.X. (2003). Singularities of parallel manipulators: a geometric treatment. *IEEE Transactions on Robotics and Automation*, Vol. 19, No. 4, pp. 579-594
- Merlet, J.P. (1992). On the infinitesimal motion of a parallel manipulator in singular configurations, *Proceedings of IEEE International Conference on Robotics and Automation*, pp. 320-325, Nice, France, May, 1992
- Merlet, J.-P. (2000). Kinematics' not dead, *Proceedings of IEEE International Conference on Robotics & Automation*, pp. 1-6, San Francisco, CA, April, 2000
- Merlet, J.-P. & Daney, D. (2005). Dimensional synthesis of parallel robots with a guaranteed given accuracy over a specific workspace, *Proceedings of IEEE International Conference on Robotics and Automation*, pp. 19-22, Barcelona, Spain, April, 2005
- Merlet, J.-P. (2006). *Parallel Robots (Second Edition)*, Springer, Dordrecht, The Netherlands
- Nabat, V.; Company, O. & Krut, M. et al. (2005). Part 4: very high speed parallel robot for pick-and-place, *Proceedings of IEEE International Conference on Intelligent Robots and Systems*, pp. 553-558, Edmonton, Canada, August, 2005
- Nabat, V.; Company, O. & Pierrot, F. (2006). Dynamic modeling and identification of Part 4, a very high speed parallel manipulator, *Proceedings of the International Conference on Intelligent Robots and Systems*, pp. 496-501, Beijing, China, October, 2006
- Parenti-Castelli, P. & Di Gregorio, P. (20010). Real-time actual pose determination of the general fully parallel spherical wrist, using only one extra sensor. *Journal of Robotic Systems*, Vol. 18, No. 12, pp. 723-729
- Pennock, G.R. & Kassner, D.J. (1990). Kinematic analysis of a planar eight-bar linkage: application to a platform-type robot, *ASME Proceedings of the 21th Biennial Mechanism Conference*, pp. 37-43, Chicago, September, 1990
- Pierrot, F. & Company, O. (1999). H4: a new family of 4-dof parallel robots, *Proceedings of the 1999 IEEE/ASME International Conference on Advanced Intelligent Mechatronics*, pp. 508-513, Atlanta, USA, September, 1999

- Pottmann, H.; Peterzell, M. & Ravani, B. (1999). An introduction to line geometry with applications. *Computer Aided Design*, Vol. 31, pp. 3-16
- Reboulet, C. & Robert, A. (1985). Hybrid control of a manipulator with an active compliant wrist, *The 3rd International Symposium of Robotics Research*, pp. 76-80, Gouvieux, France, October, 1985
- Renaud, P.; Andreff, N. & Marquet, F. et al.. (2003). Vision-based kinematic calibration of a H4 parallel mechanism. *Proceedings of the IEEE International Conference on Robotics & Automation*, pp. 1191-1196, Taipei, Taiwan, September, 2003
- Robotics Department of LIRMM. H4 with rotary drives: a member of H4 family, dedicated to high speed applications. http://www.lirmm.fr/w3rob/SiteWeb/detail_resultat.php?num_resultat=7&num_topic=1&num_projet=1&num_activite=3
- Rolland, L. The manta and the kanuk: novel 4-dof parallel mechanisms for industrial handling. *ASME Dynamic Systems and Control Division, IMECE'99 Conference*, pp. 831-844, Nashville, USA, November 1999
- Romdhane, L.; Affi, Z. & Fayet, M. (2002). Design and singularity analysis of a 3-translational-DOF in-parallel manipulator. *ASME Journal of Mechanical Design*, Vol. 124, pp. 419-426
- Ryu, J. & Cha, J. (2003). Volumetric error analysis and architecture optimization for accuracy of HexaSlide type parallel manipulators. *Mechanism and Machine Theory*, Vol. 38, pp. 227-240
- Steward, D. (1965). A platform with 6 degrees of freedom. *Proceedings of the Institution of Mechanical Engineers*, Vol. 180, Part 1, No. 15, pp. 371-386, British
- St-Onge, B.M. & Gosselin, C.M. (2000). Singularity analysis and representation of the general Gough-Stewart platform. *International Journal of Robot Research*, Vol.19, No. 3, pp. 271-288
- Su, Y.X.; Duan, B.Y. & Peng, B. et al.. (2003). Singularity analysis of fine-tuning stewart platform for large radio telescope using genetic algorithm. *Mechatronics*, Vol. 13, pp. 413-425
- Tsai, L.-W. (1996). Kinematics of a three-DOF platform with three extensible limbs. *Recent Advances in Robot Kinematics*, Kluwer Academic Publishers, pp. 401-410
- Tsai, L.-W. & Joshi, S.A. (2000). Kinematics and optimization of a spatial 3-UPU parallel manipulators. *ASME Journal of Mechanical Design*, Vol. 122, No.4, pp. 439-446
- Wolf, A. & Shoham, M. (2003). Investigation of parallel manipulators using linear complex approximation. *ASME Journal of Mechanical Design*, Vol. 125, No. 3, pp. 564-572
- Wu, J.; Yin, Z. & Xiong, Y. (2006). Singularity analysis of a novel 4-dof parallel manipulator H4. *International Journal of Advanced Manufacturing and Technology*, Vol. 29, pp. 794-802
- Zlatanov, D.; Fenton, R.G. & Benhabib, B. (1994). Singularity analysis of mechanism and robots via a motion-space model of the instantaneous kinematics. *Proceedings of IEEE International Conference on Robotics and Automation*, pp. 980-991, San Diego, CA, May, 1994

- Zlatanov, D.; Benov, I.A. & Gosselin, C.M. (2002). Constraint singularities of parallel mechanisms, *Proceedings of the IEEE International Conference on Robotics and Automation*, pp. 496-502, Washington DC, May, 2002
- Zobel, P.B., Di Stefano, P. & Raparelli, T. (1996). The design of a 3 dof parallel robot with pneumatic drives, *Proceedings of the 27th International Symposium on Industrial Robot*, pp. 707-710, October, 1996, Milan

IntechOpen

IntechOpen



Parallel Manipulators, towards New Applications

Edited by Huapeng Wu

ISBN 978-3-902613-40-0

Hard cover, 506 pages

Publisher I-Tech Education and Publishing

Published online 01, April, 2008

Published in print edition April, 2008

In recent years, parallel kinematics mechanisms have attracted a lot of attention from the academic and industrial communities due to potential applications not only as robot manipulators but also as machine tools. Generally, the criteria used to compare the performance of traditional serial robots and parallel robots are the workspace, the ratio between the payload and the robot mass, accuracy, and dynamic behaviour. In addition to the reduced coupling effect between joints, parallel robots bring the benefits of much higher payload-robot mass ratios, superior accuracy and greater stiffness; qualities which lead to better dynamic performance. The main drawback with parallel robots is the relatively small workspace. A great deal of research on parallel robots has been carried out worldwide, and a large number of parallel mechanism systems have been built for various applications, such as remote handling, machine tools, medical robots, simulators, micro-robots, and humanoid robots. This book opens a window to exceptional research and development work on parallel mechanisms contributed by authors from around the world. Through this window the reader can get a good view of current parallel robot research and applications.

How to reference

In order to correctly reference this scholarly work, feel free to copy and paste the following:

Jinbo Wu and Zhouping Yin (2008). A Novel 4-DOF Parallel Manipulator H4, Parallel Manipulators, towards New Applications, Huapeng Wu (Ed.), ISBN: 978-3-902613-40-0, InTech, Available from:
http://www.intechopen.com/books/parallel_manipulators_towards_new_applications/a_novel_4-dof_parallel_manipulator_h4

INTECH
open science | open minds

InTech Europe

University Campus STeP Ri
Slavka Krautzeka 83/A
51000 Rijeka, Croatia
Phone: +385 (51) 770 447
Fax: +385 (51) 686 166
www.intechopen.com

InTech China

Unit 405, Office Block, Hotel Equatorial Shanghai
No.65, Yan An Road (West), Shanghai, 200040, China
中国上海市延安西路65号上海国际贵都大饭店办公楼405单元
Phone: +86-21-62489820
Fax: +86-21-62489821

© 2008 The Author(s). Licensee IntechOpen. This chapter is distributed under the terms of the [Creative Commons Attribution-NonCommercial-ShareAlike-3.0 License](https://creativecommons.org/licenses/by-nc-sa/3.0/), which permits use, distribution and reproduction for non-commercial purposes, provided the original is properly cited and derivative works building on this content are distributed under the same license.

IntechOpen

IntechOpen